5.7.3 Chemical Sensors

Depending on the kind of recognition element, a sensor may be biochemical or chemical. In the chemical category, the recognition element is non-biological in origin and is synthesized in the laboratory. There are several chemical sensors which use SAMs and utilize a variety of properties. Electrochemical, capacitance, plasmon resonance and mass are the most common properties utilized for transduction of the recognition event.

One of the most common sensing events is the quantitative detection of transition metal ions, especially in presence of other ions. The detection of Cu(II) in presence of Fe(III) is an example. The four-coordination preference of Cu^{2+} can be provided by attaching a tetradentate ligand and the other end of the molecule can be anchored onto the gold surface. The sensor sites can be kept separated by preparing a mixed SAM. The presence of other ions does not influence the detection as they do not get attached to the electrode surface. A variety of ligands and metal ions can be used to implement this approach.

Molecular imprinting is another approach that has been developed for sensing. Here the shape of a molecule is imprinted on the monolayer surface and when the location is occupied by the analyte molecule, it is recognized as a sensing event. In one of the approaches demonstrated, a mould for the analyte barbituric acid, in the form of thiobarbituric acid, is made to bind the surface. The shape is imprinted on the surface by co-adsorbing another monolayer forming thiols. When the analyte molecule is exposed to the surface, it can bind to the cavities imprinted on the surface. This binding event changes the capacitance of the surface. Several molecules such as cholesterol, barburates, quinines, etc. have been detected in this way (Ref. 30).

5.7.4 pH Sensing is Ion Sensing

SAMs have been used for pH sensing by several investigators. The general approach is to have two electroactive species on the monolayer surface. While one is pH-sensitive, the other is insensitive and acts as a reference. This is seen in the case of quinine and ferrocene, both of which are immobilized on the monolayer surface. While in the first, the oxidation and reduction shift linearly with pH, the second does not show any response to pH. It is also possible to make the pH-independent electrochemistry of ferrocene pH-dependent by having a bifunctional molecule. In one of the approaches used, a ferrocene carboxylic acid is linked to the surface through a –S linkage. The oxidized state of ferrocene is stabilized by the deprotonation of the carboxylic acid group, which makes the redox chemistry of ferrocene pH-dependent.

5.7.5 Corrosion Prevention

When used as coatings, SAMs offer corrosion resistance. In this regard, several monolayers have been made on surfaces such as Au, Cu, Fe, etc. The chain length of the molecule has to be long enough to offer effective protection. The monolayer coating is inadequate in offering complete protection against ion penetration. The permeability of ions through the assembly poses a serious problem, thereby necessitating

an additional coating on the monolayer. An approach that has been tried to resolve this problem is to make a siloxane polymer of the SAM.

5.7.6 Other Areas

Self-assembled monolayers on a gold surface constitute an ideal system for practising fundamental studies related to the electron transfer process. The electrode surface used for this purpose is modified with electoactive monolayers through self-assembly. The attachment of thiols with the active terminal group allows further derivatization through classical organic reactions. In one attempt, cycloaddition was also used to derivatize a surface modified with thiol containing azide at the termini (Fig. 5.18).

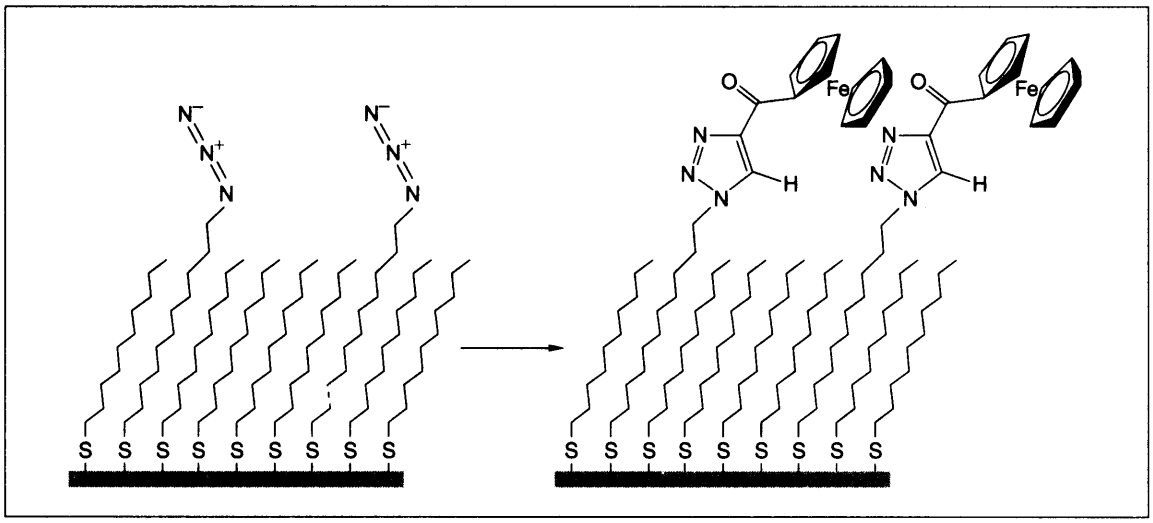

Fig. 5.18: *Electrode surface before and after cycloaddition. Reprinted with permission from Collman, et al. (Ref 31). Copyright (2004) American Chemical Society.*

Chemical force microscopy (CFM) combined with chiral discrimination by a molecule can be used to distinguish different chiral forms of the same molecule. In this technique, an AFM tip is functionalized with a chiral molecule. This chiral probe is then used to discriminate between the two chiral forms of the same molecule on a surface. The gold-coated AFM tip is functionalized with a chiral probe by using acylated phenyl glycine modified with alkanethiol. The changes in the friction or adhesion forces are used to distinguish between the two enantiomers of mandelic acid.

5.7.7 Wetting Control

The wetting properties of a surface can be modified, to a great extent, by coating it with a monolayer of molecules. This is one of the important applications of SAMs. A low coverage surface is made intentionally

by the self-assembly of alkanethiol with a bulky end group on an Au(111) surface. The end group is then hydrolyzed to form a carboxy terminated monolayer with low surface coverage. The carboxylate groups generated by the hydrolysis can be attracted to the gold surface by applying an electric field. Thus the surface can now be made hydrophilic or hydrophobic by changing the electrochemical potential. The working of the sensor is schematically shown in Fig. 5.19 (Plate 4).

5.7.8 Molecular Electronics

SAMs are also used to make electrical contacts. By using a self-assembled monolayer of dithiol on gold, one can make a surface with pendent thiol groups and can also attach a gold nanoparticle. This attachment with a covalent linkage showed four orders of magnitude higher current than when the nanoparticle was physisorbed on the SAM surface at the same tip bias voltage. This showed that monolayer-based electrical contacts are feasible. In various studies, different kinds of interactions such as van der Waals, hydrogen bonding and covalent interactions have been made between monolayers attached to metallic surfaces such as gold and mercury. These studies have shown that the electron transfer rates increased in the order, van der Waals > hydrogen bonding < covalent.

In all these experiments, it is necessary to make a contact. This is done through monolayers. The experimental protocol is illustrated in Fig. 5.20. In the experiment, a nanoparticle solution is exposed to a monolayer making nanoparticles sit on the monolayer. The current flowing between the tip and the surface is measured at a bias voltage.

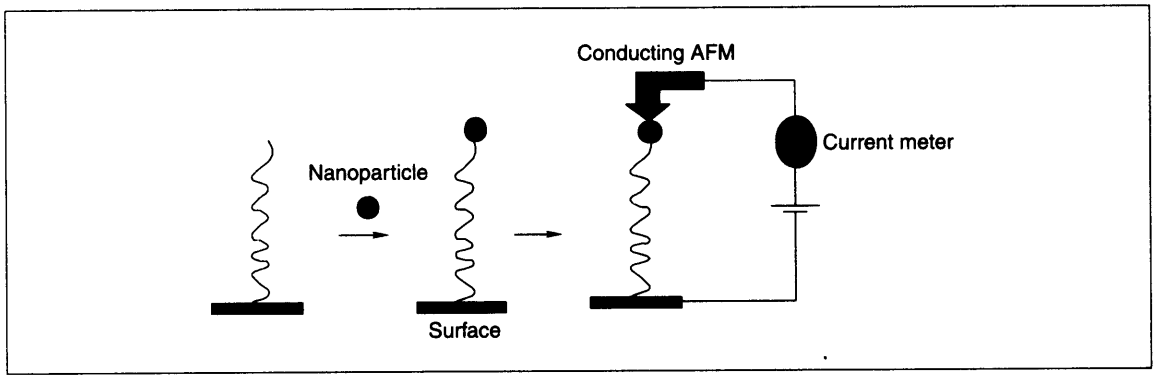

Fig. 5.20: *Experimental approach for making electrical contact to a nanoparticle.*

5.7.9 Templates

SAMS are excellent templates on which nanofabrication can be done. A given structure can be produced on the surface by using a number of methodologies. Various nanoscopic objects can be used for producing a structure. Several of these objects are detailed below.

Nanoparticles Monolayer-protected nanoparticles (see Chapter 8) are new kinds of materials. In this class of systems, monolayers are grown on the surface of nanoparticles of metals, semiconductors and insulators. The monolayer protection allows the nanoparticle to preserve its size and shape. Through a judicious choice of the functionality on the nanoparticle surface, one can bind the material on to an SAM in a well-defined fashion. The nanoparticle surface can be coated with various molecules having additional properties. The chemistry discussed on the planar monolayer surface can be eminently done on the nanoparticle surface as well. One of the important aspects in the use of nanoparticles is that with monolayer functionalization, nanoparticles can be incorporated in any matrix such as polymers. It is also possible to attach nanoparticles on solid surfaces through a monolayer anchor. This allows one to produce device structures with nanoparticles.

Nanotubes By functionalizing carbon nanotubes, one can attach them to SAMs through specific chemistry. This facilitates the arrangement of aligned nanotubes on monolayer surfaces. In this way, nanotubes can be made available on stable supports. They can be used as devices for applications such as field emission.

Crystal Growth As mentioned earlier, SAMs can nucleate crystal growth and such low temperature chemical routes are important for making ultra-thin layers of materials. By creating a functional molecular surface at specific locations, it is possible to grow another material at these locations. Several examples of these are known. The formation of tetragonal zirconia on SAMs has been reported (Ref. 33). In Fig. 5.21 a SEM image of ZrO_2 crystals grown on a SAM is shown. The crystals are highly faceted, and signify one of the very early examples of low temperature growth of ordered materials. The SAMs act as templates on which initial nucleation occurs. There are also examples of this kind of assisted growth on metal nanoparticles, wherein a ZrO_2 shell is grown on silver nanoparticles by solution chemistry (Ref. 34).

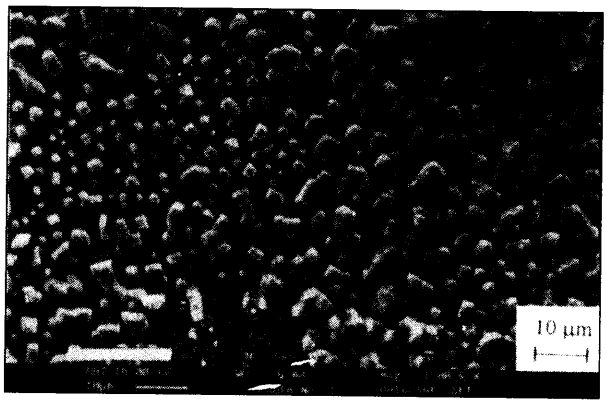

Fig. 5.21: *Scanning electron micrograph of tetragonal ZrO_2 grown on self-assembled monolayers. From Bandyopadhyay, et al. (Ref. 33). Used with permission from the author.*

By patterning an SAM with mercaptohexanoic acid (MHA) and the balance with mercaptohexanol (MCH) it has been shown that calcite crystals are grown selectively at locations of MHA instead of MCH (Ref. 35). Several other materials have also been grown in this way.

Polymers One can build polymers on an organized structure. The variety in polymeric structures is diverse so that almost anything can be grown on a SAM surface through an appropriate choice of precursors.

Complex Molecules One can also think of placing biological molecules at specific locations just as in materials chemistry. The most common biomaterials are proteins and placing them on metal surfaces is important. However, proteins placed directly on surfaces get denatured, which is why placing them on SAMs is a feasible alternative. The problem, however, is that SAMs have a non-specific affinity for proteins, which needs to be controlled. Ethylene glycol units on the surface prevent non-specific protein adsorption and SAMs with 4 to 7 poly(ethyleneglycol) units are used for this purpose. Specific thiolated monolayers can be grown on surfaces and the protein can have a biorecognition function. Such an approach can be used to adhere cells onto monolayers. This is mediated by proteins of the extracellular matrix (ECM) such as fibronectin and collagen. These proteins can be anchored to surfaces by using patterned monolayers. All the unpatterned region of the SAM is covered with poly(ethylenegycol) monolayer so that no protein adsorption occurs. Cells can then be attached to the protein modified sites. The size of the islands affects the cell growth. This kind of capability, along with the spatial control that is possible in monolayer growth, will make it possible to have lab on a chip.

Layer-by-layer-Structure SAMs involve growing layers. If such monolayers can be grown one over the other, step by step, microscopic thickness can be generated. For achieving this, it is important to have the link the monolayers through covalent chemistry. In one such approach, a benzenedimethane thiol (BDMT) monolayer was linked to another thiol through the covalent chemistry of the pendent thiol group of the BDMT monolayer (Ref. 36).

Review Questions

1. Why are these monolayers referred to as, 'self-assembled'? Are there 'force-assembled' monolayers?
2. What are the various aspects which determine the stability of a monolayer?
3. Why self assembled monolayers are ideal systems for probing fundamental phenomena? State a few such phenomena not described here.
4. Why SAMs are difficult to study?
5. Propose a few other monolayer systems other than alkane thiols on gold.
6. How do we study the kinetics of self organization by experimental means?
7. Monolayers are crystalline assemblies. How does one study the changes in the crystalline order, especially as a function of temperature?

8. Suggest a few uses of monolayers not described in this chapter.
9. Are there day to day examples of monolayers?
10. Suggest a method to study the strength of single chemical bonds using monolayers.

References

1. Atomic and Nano Technology, IBM Research, http://www.research.ibm.com/atomic.
2. Langmuir, I., *J. Am. Chem. Soc.*, **39** (1917), p. 1848.
3. Blodgett, K., *J. Am. Chem. Soc.*, **57** (1935), p. 1007.
4. Bigelow, W.C., D.L. Pickett and W.A. Zisman, *J. Colloid Interface Sci.*, **1** (1946), p. 513.
5. Nuzzo, R.G. and D.L. Allara, *J. Am. Chem. Soc.*, **105** (1983), p. 4481.
6. Ulaman, A., (1991), *An Introduction to Ultra-thin Organic Films from Langumir-Blodgtt to Self-Assembly*, Academic Press, London.
7. Ulman, A., *Chem. Rev.*, **96** (1996), p. 1533.
8. Chidsey, C.E.D., G.Y. Liu, P. Rowntree and G. Scoles, *J. Chem. Phys.*, **91** (1989), p. 4421.
9. Dubois, L.H. and R.G. Nuzzo, *Annu. Rev., Phys. Chem.*, **43** (1992), p. 437.
10. Sheen, C.W., J.X. Shi, J. Martensson, A.N. Parikh and D.L. Allara, *J. Am. Chem. Soc.*, **114** (1992), p. 1514.
11. Alves, C.A., E.L. Smith and M.D. Porter, *J. Am. Chem. Soc.*, **114** (1992), p. 1222.
12. Schreiber, F., A. Eberhardt, T.Y.B. Leung, P. Schwartz, S.M. Wetterer, D.J. Laurich, L. Berman, P. Fenter, P. Eisenberger and G. Scoles, *Phys. Rev.*, **B 57** (1998), 12476.
13. Poirier, G.E., M.J. Tarlov, *Langmuir*, **10** (1994), 2853.
14. Schreiber, F. *Proc. Sur. Sci.*, **65** (2000), 151.
15. Sandhyarani, N. and T. Pradeep, *Vacuum*, **49** (1998), p. 279.
16. Sandhyarani, N. and T. Pradeep, *Chem. Phys. Lett.*, **338** (2001), pp. 33–36.
17. Bensebaa, F., T.H. Ellis, A. Badia and R.B. Lennox, *J. Vac. Sci. Technol. A*, **13** (1995), p. 1331.
18. Satjapipat, M., R. Sanedrin, and F.M. Zohu, *Langmuir*, **17** (2001), p. 7637.
19. Behm, J.M., K.R. Lykke, M.J. Pellin and J.C. Hemminger, *Langmuir*, **12** (1996), p. 2121.
20. Younkin, R., K.K. Berggren, K.S. Johnson, M. Prentiss, D.C. Ralph and G.M. Whitesides, *Appl. Phys. Lett.*, **71** (1997), p. 1261.
21. Liu, G.Y., S. Xu, and l. Qian, *Acc. Chem. Res.*, **33** (2000), p. 457.
22. Xia, Y. and G.M. Whitesides, Angew. *Chem. Int. Ed.*, **37** (1998), p. 551.
23. Piner, R.D., J. Zhu, F. Zu, S. Hong and C.A. Mirkin, *Science*, **283** (1999), p. 661.

24. Schierbaum, R.D., T.E. Weiss, E.U. Thoden van Velzen, J.F.J. Engbersen, D.N. Reinhoudt and W. Göpel, *Science*, **265** (1994), p. 1413.
25. Shipway, N., E. Katz and I. Willner, *Chemphyschem*, **1** (2000), p. 18.
26. Levicky, R., T.M Herne, M.J. Tarlov and S.K. Satija, *J. Am. Chem. Soc.*, **120** (1998), 9787.
27. Fung, Y.S. and Y.Y. Wong, *Anal. Chem.*, **73** (2001), p. 5302.
28. Cornell, B.A., V.L.B. Braach–Maksvytis, L.G. King, P.D.J. Osman, B. Raguse, L. Wieczorek and R.J. Pace, *Nature*, **387** (1997), p. 580.
29. Lucas, S.W. and M.M. Harding, *Anal. Biochem.*, **282** (2000), p. 70.
30. Mirsky, V.M., T. Hirsch, S.A. Piletsky and O.S. Wolfbeis, *Angew. Chem.-Int. Ed.*, **38**, (1999), p. 1108.
31. Collman, J.P., N. K. Devaraj and E.D. Chidsey, *Langmuir*, **20** (2004), p. 1051.
32. Lahann, J., S. Mitragotri, T. Tran, H. Kaido, J. Sundaran, S. Hoffer, G.A. Somorjai and R. Langer, *Science*, **299** (2003), p. 371.
33. Bandyopadhyay, K., S.R. Sainkar and K. Vijayamohanan, *J. Am. Cer. Soc.*, **82** (1999), p. 222.
34. Eswaranand, V. and T. Pradeep, *J. Mat. Chem.*, **12** (2002), p. 2421.
35. Aizenberg, J., A.J. Black and G.M. Whisides, *Nature*, **398** (1999), p. 495.
36. Murty, K.V.G.K., M. Venkataramanan and T. Pradeep, *Langmuir*, **14** (1998), p. 5446.

Additional Reading

1. Pradeep, T. and N. Sandhyarani, *Pure and Appl. Chem.*, **74** (2002), pp. 1593–1607.
2. Sandhyarani, N. and T. Pradeep, *Int. Rev. Phys. Chem.*, **22** (2003), pp. 221–262.
3. J.J. Gooding (2004) in *Encyclopaedia of Nanoscience and Nanotechnology*, **1**, pp. 17–49, H.S. Nalwa, (ed.) American Scientific Publishers.

Chapter 6

Gas Phase Clusters

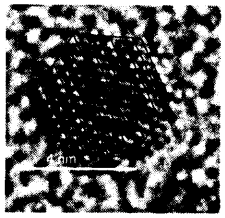

Clusters belong to a new class of systems and are studied to understand several aspects related to the science of nanomaterials. Nanoparticles are nucleated at the cluster stage and it is important to understand these systems in the naked state using mass spectrometry in order to know the origin of molecular and electronic structure in bulk systems. Almost everything forms clusters and the diversity in cluster systems is vast. The methods of preparation of clusters and their diverse variety are discussed in this chapter. While exploring clusters, scientists have discovered new molecules such as C_{60}. The chemistry of clusters in the gas phase still constitutes an active area of investigation.

Learning Objectives

- Why do you study clusters?
- How do you make them and study them?
- What are the commonly found cluster types?
- What are the basic techniques of gas phase cluster spectroscopy?
- How can one understand the properties of clusters?

6.1 Introduction

Clusters belong to a new category of materials; in size they fall between bulk materials and their atomic or molecular constituents. Sometimes they are considered to constitute a new form of matter, as their properties are fundamentally different from those of discrete molecules and bulk solids. They are systems of bound atoms or molecules, existing as an intermediate form of matter, with properties that lie between those of atoms (or molecules) and bulk materials. Depending on the kind of constituent units, they are called either atomic or molecular clusters. The term, 'molecular clusters' also implies clusters which behave like super molecules. Clusters include species existing only in the gas phase or in the condensed phase or in both. Clusters identified first in the gas phase have been synthesized later in the condensed phase and vice versa. They can have a net charge (ionic clusters) or no charge (neutral clusters) at all. The finite aggregates of atoms or molecules constituting clusters are bound by forces which may be metallic, covalent,

ionic, hydrogen bonded or van der Waals in character and can contain up to a few thousand atoms (called the *nuclearity* of the cluster). As a result, they have regular shapes (such as icosahedra). However, they also exist in a spherical shape. Usually, one can distinguish between different types of clusters by the nature of the forces between the atoms, or by the principles of spatial organization within the clusters. Clusters containing a well-defined number of transition metal atoms have unique chemical, electronic and magnetic properties, which vary dramatically with the number of constituent atoms, the type of element and the charge on the cluster. Clusters differ from bulk materials in terms of the presence of a magic number of atoms or molecules they contain. Magic numbers signify electronic and structural stability. Although this chapter is written from the perspective of gas phase spectroscopy, the reader may note that clusters are also made in the condensed phase. Examples of such clusters include molecules containing metal clusters within, with various kinds of protecting ligands, which are being investigated in several labs including ours. These studies are even more exciting now as such clusters containing a few atoms of noble metals, such as Au_{25} for example, can be made in the laboratory as a bulk powder, stored and investigated over long periods. In essence, they are similar to many laboratory chemicals.

As shown in Fig. 6.1 clusters can be depicted as a state between isolated atoms or bulk solid. What is also implied is that it is possible to get them from either side, from atoms or molecules or from both.

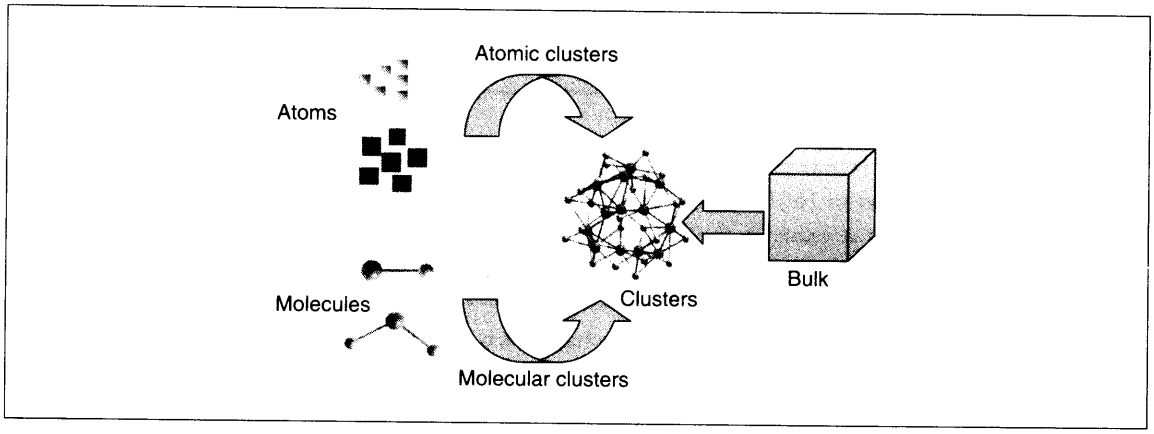

Fig. 6.1: *Schematic representation of cluster placed in between atom, molecule and bulk material. From left to right the dimension of the constituent matter increases. Clusters can be produced from atomic or molecular constituents or from the bulk material. The variously colored balls are all different kinds of atoms. In relation to the dimensions of atoms and the cluster shown, the material should be a thousand times larger than the one depicted.*

From a general perspective, there are two broad reasons why we investigate clusters. There are several associated reasons as well. 1. As clusters bridge the gap between molecules and materials, the evolution in properties of molecules as they become materials can be understood by investigating clusters. 2. Properties such as chemical reactivity and catalysis depend strongly on specific geometry, electronic structure, etc., and clusters help us to understand such fundamental phenomena. Such understanding can make large economic impact, for example, in terms of making the most appropriate, greener, cleaner and economical catalyst.

One can distinguish the properties of atoms molecules of clusters as listed in Table 6.1.

Table 6.1: *Difference between atom, molecule, clusters and bulk materials*

Property	Atom/Molecule	Cluster	Bulk material
Size of constituting entities	Few Angstroms (Å)	Angstrom (Å) to nanometer (nm)	Microns to higher
Number of constituents (n)	1 for atom, many for molecule	2 to several thousands	Infinite
Electronic structure	Confined (quantized)	Confined (quantized)	Continuous
Geometric structure	Well-defined and predictable	Well-defined and predictable	Crystal structure decides
Example	Na/NaCl/C_6H_6	C_{60}, $(NaCl)_n$	Bulk gold, silver

6.2 History of Cluster Science

The importance of clusters was first proposed by the Irish-born chemist Robert Boyle in his book, *The Sceptical Chymist* published in 1661 (Ref. 1). In it Boyle was critical of Aristotle's four element theory of matter and proposed that it exists in the form of 'corpuscles'. He thought about it, "minute masses or clusters that were not easily dissipable into such particles that composed them." 'Clusters' for him were not collections of atoms or molecules as both were unknown then.

During the last several decades, cluster science has grown to become a field of interdisciplinary study. Improvement in experimental techniques such as mass spectrometry and advancement in computational power (and methods) have increased the interest in cluster science. After the discovery of buckminsterfullerene, C_{60}, the field of cluster science witnessed an enormous growth. The use of clusters goes back to several centuries. Examples of application include photography (AgBr clusters in films) and glass works (for staining); see Chapter 1 for more details. There are several eastern societies which used small particles in medicines. Rayleigh recognized that colors of stained glasses are due to the scattering of light by small metal particles, clusters of atoms embedded in the glass.

6.3 Cluster Formation

In any material, there are atoms on the surface. But the number of surface atoms is very small in comparison to the bulk. If one takes a one cm^3 metal block, there are about 2×10^{23} atoms in it, assuming a radius of

1 Å for the atom. On the surface of this cube, there are only about 1.5×10^{16} atoms. The fraction of surface atoms is one in a million and therefore they do not make measurable influence in the properties investigated. However, in the case of a cluster, this fraction can be of the order of one and that makes significant difference in the properties. Assuming a spherical cluster, the fraction of surface atoms is (number of atoms on the surface/total number of atoms), $F = 4/n^{1/3}$, where n is the total number of atoms. One can see that, $F = 0.3$ for $n = 1{,}000$, $F = 0.2$ for $n = 10{,}000$ and $F = 0.04$ for $n = 1{,}000{,}000$. The surface atoms are unsatisfied in their valencies and they are extremely reactive due to this reason. Therefore, many of the clusters cannot be kept in the free state. They have to be made *in-situ,* in experimental apparatus where the properties are investigated. Therefore, almost all the studies are conducted in vacuum or in presence of rare gases.

Gas phase clusters are generated in cluster sources. There are many kinds of cluster sources. Some of them are listed below.

- Laser vaporization-flow condensation source
- Pulsed arc cluster ion source
- Laser ablation cluster source
- Supersonic (free jet) nozzle source
- Knudsen cell (effusive source)
- Ion sputtering source
- Magnetron sputtering source
- Gas aggregation/Smoke source
- Liquid metal ion source

Some of the more common methods are described below. Additional reading material listed at the end of the chapter may be consulted for more details.

6.3.1 Laser Vaporization

The laser vaporization source is a pulsed cluster source which is used to produce small- and medium-sized clusters. The resultant cluster may be formed from any element or compound. This method typically combines laser ablation and supersonic jet expansion. In the laser vaporization source, vapor is generated by pulsed laser ablation of a rod of the starting material. An intense pulsed *UV* laser is used here (typically third or fourth harmonic of *Nd:YAG*). Each 10 ns pulse vaporizes 10^{14}–10^{15} atoms per mm^2 of the target. Since the use of lasers for cluster generation also leads to ionization, this source also generates neutral, cationic and anionic clusters which can be investigated directly by mass spectrometry, without post-ionization. In fact what is produced by laser evaporation is a plasma. Pulsing helps in (1) to get an intense light capable of evaporation of materials directly breaking their bonds in the lattice, (2) produces a pulse of clusters suitable for time of flight analysis and (3) pulsed laser firing and subsequent expansion of the evaporated plasma into vacuum is generally done in presence of a carrier gas, which is also pulsed, reducing the pumping requirements.

6.3.2 Pulsed Arc Cluster Ion Source

Pulsed arc cluster ion sources (PACIS) are related to laser vaporization sources. Instead of the laser here the cluster precursor is vaporized by an intense electrical discharge. Cluster beams generated in this way are significantly more intense in comparison to laser vaporization. Nearly 10 per cent of the clusters formed by using this technique are charged and again, post ionization is not necessary for mass analysis.

6.3.3 Supersonic (Free Jet) Nozzle Sources

Supersonic nozzle sources are of two main types, unseeded and seeded. In the first type, clusters of inert gases, molecules and low boiling metals (e.g. Hg) are formed. In the other type, the metal is vaporized (with a vapor pressure of 10–100 mbar) in an oven and the vapor is mixed with (seeded) an inert carrier gas at a pressure of several atmospheres (10^5–10^6 pa) at a temperature of 77–1500 K. The metal/carrier gas mixture is then expanded through a nozzle (with diameter of 0.03–0.1 mm) into high vacuum (10^{-1}–10^{-3} Pa), which creates a supersonic beam. Nozzles with rectangular opening have been used to generate two-dimensional cluster beams (normally they have a disk-like cross section), which are necessary for certain studies. The cluster growth stops at least immediately after the nozzle exit, when the vapor density reduces drastically. Such sources produce intense continuous cluster beams of narrow energy spread, suitable for high resolution spectroscopy. Seeding produces large clusters while in the absence of a carrier gas, smaller clusters (>10 atoms) are formed. Intensity of the beam and the smaller energy spread are the significant aspects of this kind of sources.

6.3.4 Gas-Aggregation or Smoke Sources

The source utilizes the property of aggregation of atoms in inert media. The vapors generated by one of the several means are introduced into a cold inert gas at a high pressure of the order of 1 torr. The species, originally at a high temperature, are thermalized. The gas phase is supersaturated with the species and they aggregate. These sources produce continuous beams of clusters of low-to-medium boiling (<2000 K) metals. By controlling the kinetics of quenching and aggregation, various cluster sizes can be produced.

6.3.5 Knudsen Cell

The Knudsen cell produces a continuous, low flux beam of clusters. The velocity of the species is low (subsonic). In the cell having a small aperture, a volatile solid or liquid is heated; the cell itself is held in a vacuum vessel. In design, this is similar to a smoke source. At the low vapor pressures produced, their mean free path is greater than the collision diameter of the aperture, as a result of which there are very few collisions before particles leave the cell. The energy resolution of the cluster beam formed in the effusive sources is poor. The angular spread is also larger. In these sources, as the aperture is small, the solid-gas

mixture is nearly at equilibrium. The cluster intensity (I) falls exponentially with an increase in the cluster nuclearity (N) according to the equation, $I(N) = ae^{-b/N}$, where a and b are parameters. The intensities in a smaller window of masses are related to the stability of the clusters. For example, in antimony, Sb_4 dominates than Sb_3 or Sb_5.

6.3.6 Liquid Metal Ion Source

These sources are primarily used to produce clusters of multiple charges, with low-melting metals. A needle held above the melting point of the metal to be studied. The tip of it is wetted with the metal and it is held at a potential. Very high electric fields at the tip of the needle (due to smaller dimension) cause the emission of a spray of tiny droplets from it. Similar sources are used as ion sources (Chapter 2). Hot, multiply charged droplets undergo evaporative cooling and fission to smaller sizes. Fission occurs as Coulomb repulsion between the charges become larger than the binding energy of the drop itself.

In addition to the above sources sputter sources are used in which a high energy ion beam is used to sputter atoms, ions and clusters from a surface. A schematic illustration of various cluster sources is given in Fig. 6.2.

6.4 Cluster Growth

Cluster growth occurs in two stages.

Nucleation The nucleation can be homogeneous or heterogeneous. Heterogeneous implies the nucleation occurs on foreign objects, dust particles, etc. In it, collision between like or unlike atoms occurs such that the thermal energy is lower than the binding energy of the species formed. Dimer formation occurs when the third body involved in the collision removes the excess internal energy as kinetic energy.

$$A + A + A\,(KE_1) \rightarrow A_2 + A\,(KE_2 > KE_1), \text{like molecules}$$

$$A + A + B\,(KE_1) \rightarrow A_2 + B\,(KE_2 > KE_1), \text{un-like molecules}$$

The dimer acts as a seed for further condensation and additional growth occurs.

Growth Initial growth occurs by the aggregation of atoms or molecules one at a time. Coalescence of clusters results in the formation of larger clusters.

$$A_N + A \rightarrow A_{N+1}$$

$$A_N + A_M \rightarrow A_{N+M}$$

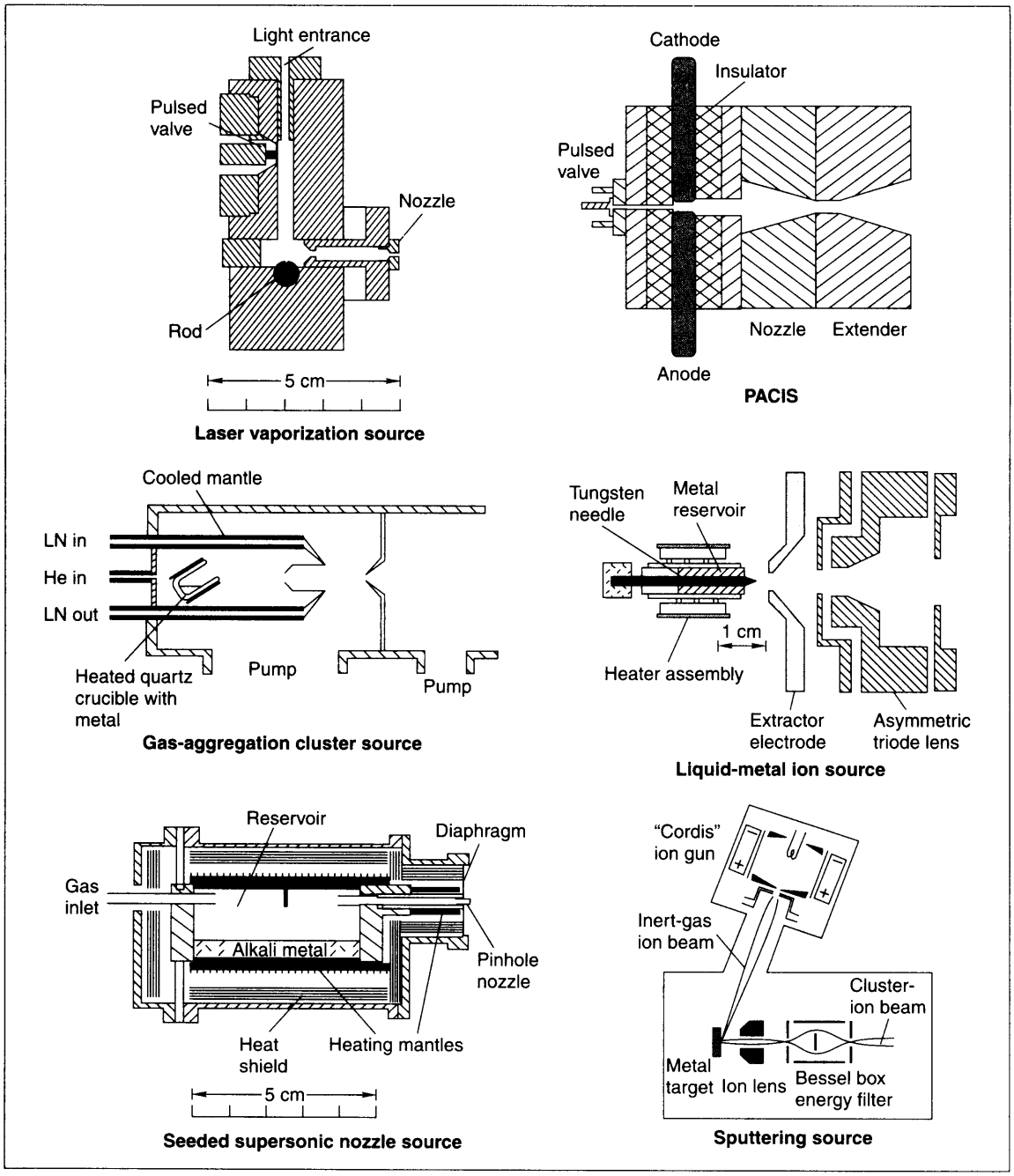

Fig. 6.2: *Various clusters sources. Reprinted with permission from, W.A. de Heer. (1993) Rev. Mod. Phys., 65, 611. Copyright (1993) by the American Physical Society.*

6.5 Detection and Analysis of Gas Phase Clusters

The formed clusters can exist as neutrals or ions (both positively and negatively charged). Various mass spectrometers are used to detect the ionic clusters. The clusters which exist in solid or in liquid state can be analyzed by several spectroscopic, microscopic or diffraction techniques. Here we will discuss the mass spectrometric studies on clusters, because we are focusing only on gas phase clusters.

Mass spectrometers are unique devices used to study the exact constitution of the clusters which exist in the gas phase. From the mass we can easily calculate the empirical formula of the cluster. Wien filter, time of flight (TOF), quadrupole mass filter (QMF), and ion cyclotron resonance (ICR) are the normal kinds of mass spectrometric techniques used to study clusters (although magnetic sector instruments can also be used). These techniques are briefly discussed below.

6.5.1 Wien Filter

This is a low resolution ($\Delta m/m \sim 10^{-2}$), low mass range (less than m/z 1500) instrument. Here mass separation is accomplished using crossed homogeneous electric (E) and magnetic (B) fields, perpendicular to the ionized clusters beam, which travels along the axis of the filter (Fig. 6.3(a)). The net force acting on a charged cluster with mass M, charge Q, and velocity v vanishes if $E = Bv$. These cluster ions are accelerated by a voltage V, so that they have energy QV (where Q is the charge). In the filter, clusters with $M/Q = 2V/(E/B)^2$ are undeflected, while others with different m/z undergo deflection and are lost (Ref. 2). The undeflected cluster ions are selected and detected, after a slit. As can be seen, the mass resolution of a Wien filter depends on the velocity spread of cluster ions, the strength of the fields, and the slit width. In order to obtain high resolution, narrow slits and strong fields are required as also large acceleration potentials, which reduces the initial velocity spread.

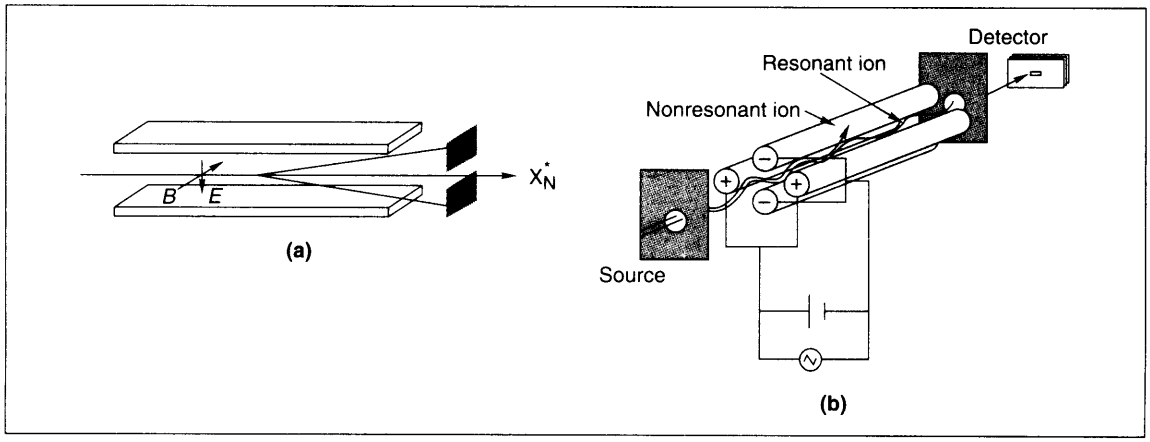

Fig. 6.3: *Schematic of (a) Wien filter and (b) quadrupole mass analyzer. Ions of one kind only pass through for a given condition.*

6.5.2 Quadrupole Mass Filter (QMF)

The QMF is the most widely used type of mass spectrometers today because of its ease of use, compactness and low cost. The principle of QMF is based on the achievement of a stable trajectory for specific ions in a hyperbolic electrostatic field. For easiness of manufacture, cylindrical rods are often used (See Fig. 6.3(b)). An idealized QMF consists of four parallel hyperbolic rods, such filters are also available. To a pair of diagonally opposite rods, a potential consisting of a *dc* voltage and a superimposed *rf* voltage is applied. To the other pair of rods, a superimposed *dc* of opposite polarity and an *rf* voltage of 180° phase shift is applied. The potential ϕ_o applied to opposite pairs of rods is given by:

$$\pm\phi_o = U + V \cos \omega t$$

where U is a *dc* voltage and $V \cos \omega t$, the time-dependent *rf* voltage in which V is the *rf* amplitude and ω, the *rf* frequency. At given values of U, V and ω, only certain ions can have stable trajectories so as to pass through and reach the detector. The various m/z values, capable of passing through the mass filter, are decided by the ratio, U/V. All the other ions will have unstable trajectories (i.e., they will have large amplitudes in x- or y-direction) and will be lost. The ion trajectory is decided by the Mathieu equations, from which Mathieu parameters a_u, and q_u can de determined.

$$a_u = a_x = -a_y = 4zU/m\omega^2 r_o^2 \qquad q_u = q_x = -q_y = 2zV/m\omega^2 r_o^2$$

where m/z is the mass-to-charge ratio of the ion and r_o, half the distance between two opposite rods. Mass scanning on a QMF means changing U and V at a constant ratio, $a/q = 2U/V$, while keeping the *rf* frequency, ω fixed. The resolving power of a QMF depends on the number of cycles experienced by an ion within the *rf* field (during its flight), which, in turn, depends on the ion velocity. Thus, the resolution will increase with an increase in mass, as ions of higher mass move with lower velocity. However, ion transmission will decrease due to the longer time the higher mass ions spend in the quadrupole. Resolution will decrease when ion is accelerated to a higher potential. The advantages of a QMF are its good transmission, high scan speed, and wide acceptance angle to facilitate high sensitivity. Due to these, it is coupled to several instruments such as gas chromatographs.

6.5.3 Time of Flight (TOF) Mass Filter

TOF has emerged as an efficient mass analyzer. There is no mass limit in this instrument. The TOF of an ion is related to its mass. A set of ions differing in mass, if accelerated through a given extraction voltage, will have varying flight times (Fig. 6.4(a)). Through the use of fast electronic circuits and by the incorporation of a reflection electric region (called reflectron) high mass resolution is possible. TOF can be used to study the dissociation of metastable clusters. A reflectron can also be used to investigate dissociation in the field-free region so that slower processes exhibited by the ion may be observed. This kind of dissociation in the field-free region is called, 'Post Source Dissociation' (PSD). Here ions are accelerated in an appropriate electric field of the order of kilovolts, and then the ions enter into the field-free region. These ions get fragmented in the reflectron region. The parent species with greater kinetic energy have a longer path

length than that of daughter ions (Fig. 6.4(b)). By subjecting the ions to different potentials, different fragments may be observed. Finally all the daughter peaks in various regions have to be combined to get the fragmentation pattern of particular clusters. Recently, many clusters and their fragments have been studied by the TOF method. This method of fragmentation is applied for the sequencing of DNA, proteins and larger peptides. Nowadays, with the advancement in electronics, the TOF has an arrangement called the Nielsen-Bradbury gate (Ref. 3). It can act as a gate which allows only a particular mass into the detector region. This can be used to study the particular clusters in the presence of many other clusters from the same source. In Fig. 6.4(b) we present a pictorial representation of the fragmentation which occurred in the reflectron region. The molecular ion peak MH^+ gets reflected and focused correctly towards the detector in the reflector region.

Possible fragmentation channels are,

$$MH^+ \rightarrow AH^+ + B$$

$$MH^+ \rightarrow A + BH^+$$

The fragments BH^+ and AH^+ are poorly focused. This happens while we apply the same potential to both the accelerating plate as well as the reflectron (what is called the mirror ratio of 1). If we change the potential in the reflectron, leaving the accelerating voltage as such, we can focus the daughter ions, instead of the parent ions, towards the detector. So by collecting various daughter ions this way, we can easily study the fragments formed from the parent ion. Combining all the daughter ion spectra we can get a complete picture of the fragmentation of the parent ion.

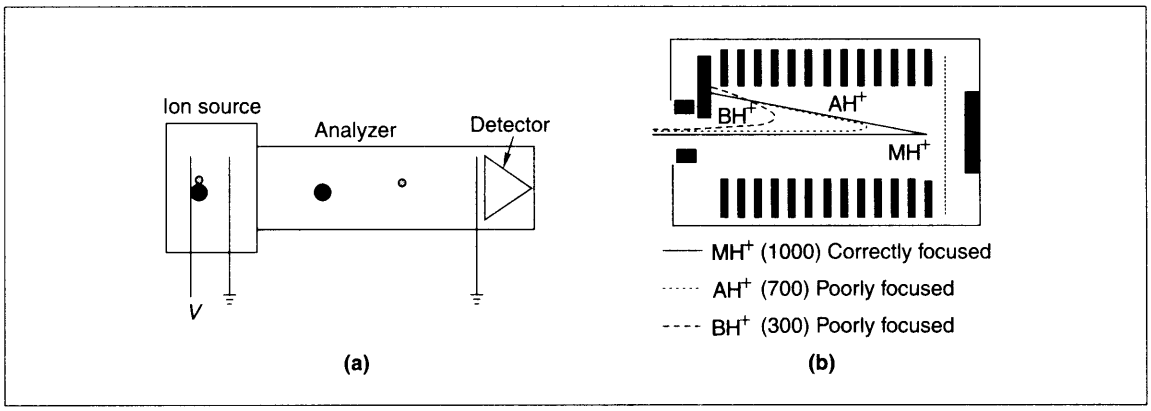

Fig. 6.4: (a) Linear TOF mass analyzer and (b) PSD mode analysis of fragments formed in the reflectron region of TOF. Masses of the ions analyzed and their trajectories are shown.

6.5.4 Ion Cyclotron Resonance

Ion cyclotron resonance (ICR) is a unique technique wherein we can, in principle, perform all the mass spectrometric studies in a single cell. They include, mass analysis, ion selection, ion interaction and product

ion mass analysis. All these are possible by a sequence of pulses which are used to initiate the various events. Ions are trapped in the cell by a combination of a static quadrupole electric field and a highly uniform magnetic field for strength, B. Due to the magnetic field, ions move at the cyclotron frequency. The equations of interest are,

$$F = zv \times B \text{ (} \times \text{ refers to a cross product)}$$

$$\omega_c = zB/2\pi m,$$

$$m/z = B/2\pi\omega_c$$

where F is the Lorentz Force felt by the ion when entering the magnetic field, v is the incident velocity of the ion, ω_c is the induced cyclotron frequency, m is the mass of the ion and z is its charge. A measurement of cyclotron frequency can be used to determine the mass-to-charge ratio (m/z) of the ions. In the ICR instrument, the cyclotron resonance frequencies are measured by exciting the ion cloud with an electrical pulse, applied on the excitation plates (Fig. 6.5). A sensitive parallel plate capacitor then picks up the electric signal from trapped ions. This signal is accumulated and then Fourier transformed. An analysis of the frequency components and their amplitudes help determine the masses and relative abundances of the ions. Unlike the other techniques, the ions are detected non-destructively which facilitate a repetitive mass analysis of the same collection of charged entities. Methods by which ions can be trapped and collided with molecules for fragmentation or reaction are also used. By combining various pulse sequences, it is possible to trap specific ions and study their chemistry. Due to the superior resolution and possibility of combining with cluster sources, and extreme sensitivity, FT-ICR is the ideal technique for cluster mass spectroscopy. However, it is highly expensive.

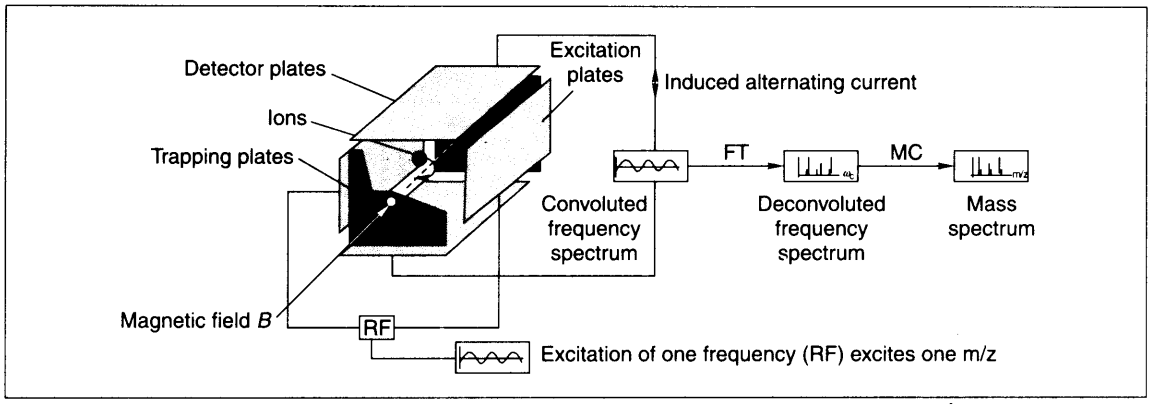

Fig. 6.5: *A schematic of FT-ICR-MS showing the ion trapping, detection and signal generation.*

6.6 Types of Clusters

Most of the elements in the periodic table form clusters. Alkali metal, coinage metal and rare gas clusters are more thoroughly investigated. Clusters can be classified according to both the type atoms of which

they are made and the nature of the bonding in these clusters. We can classify the clusters by their composition; for example, if the clusters are formed from metallic elements they are called metallic clusters. A summary of the various cluster types and properties are given in Table 6.2.

Table 6.2: *Various cluster types and their properties*

Type	Examples	Nature of binding	Binding energy/mole
Ionic clusters	$(NaCl)_n$, $(CsI)_n$	Ionic bonds (Strong binding)	~ 50–100 kcal
Covalent clusters	C_{60}, Si_n	Covalent bonding (Strong binding)	~ 20–100 kcal
Metal clusters	Au_n, Na_n, Ag_n, ...	Metallic bond (Moderate to strong binding)	~ 10–50 kcal
Molecular clusters	$(H_2O)_n$	Molecular interactions, hydrogen bonding, van der Waals, etc.	< 10 kcal
van der Waals clusters	Ar_n, Xe_n, ...	Polarization effects (Weak binding)	< 5 kcal

These are explained in greater detail below.

6.6.1 Metal Clusters

Metal clusters are formed from alkali metals, alkaline earth metals and transition metals. Metal clusters may be formed from single metallic element or from more than one metal, giving rise to intermetallic or nanoalloy clusters. Some of the metal clusters are discussed below.

Neutral sodium clusters are produced in a gas aggregation source. Metallic sodium is heated in an oven to a temperature of about 400 °C. The hot sodium vapor (partial pressure ~ 0.1 mbar) expands into a low vacuum He-atmosphere (several mbar, T ~ 77 K) where it condenses due to super-saturation. Clusters are formed and they are directed into a differentially pumped section followed by an interaction region, with additional differential pumping. The cluster velocity is related to the source conditions and ranges from 200 to 400 m/s. A typical mass spectrum of Na_n is shown in Fig. 6.6(a) (Ref. 4). As can be seen, clusters up to about 150 atoms are seen.

Various kinds of metal clusters such as silver, aluminum, copper and nickel are known. Recently such clusters are made from molecular precursors. High aggregation of silver clusters from silver trifluoroacetate can be achieved in matrix assisted laser desorption ionization (MALDI) conditions using 2-(4-hydroxyphenylazo) benzoic acid (HABA) as the matrix. MALDI-TOF mass spectrum of silver cluster is shown in Fig. 6.6(b) (Ref. 5). The clusters formed can also be nanoalloys.

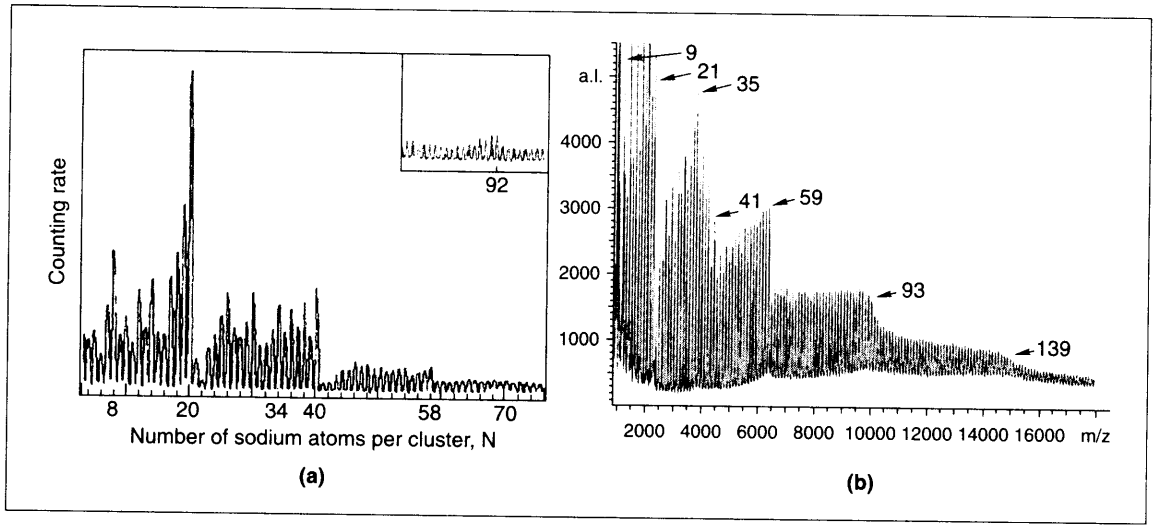

Fig. 6.6: *(a) Mass spectrum of sodium clusters, N = 4–75. Inset shows N = 75–100 region. (b) MALDI spectrum of silver clusters produced from silver trifluoroacetate. Reprinted with permission from, (a) W.D. Knight, K. Clemenger, W.A. de Heer, W.A. Saunders, M.Y. Chou, and M.L. Cohen. (1984) Phys. Rev. Lett. 52, 2141. (b) S. Kéki, L. Szilágyi, J. Török, G. Deák, and M. Zsuga. (2003) J. Phys. Chem. B, 107, 4818. Copyright (1984 and 2003) by the American Physical Society and American Chemical Society, respectively.*

6.6.2 Semiconductor Clusters

Semiconductor clusters are generated from elements which are semiconductors in nature such as silicon, carbon and germanium. The discovery of the fullerene, C_{60} a carbon cluster, stimulated researchers to explore the possibility of a number of semiconductor clusters. Carbon has the tendency to form a greater variety of clusters as compared to other elements. The bonding in these clusters is covalent in nature. The earlier carbon clusters were produced by using an electric discharge between graphite electrodes. The generated carbon clusters were detected by mass spectrometers (Ref. 6). C_{60} was discovered in such experiments in an FT-ICR, with laser desorption ionization. Fullerenes, discovered in the gas phase were later made in the condensed phase. This subject is discussed in greater detail in Chapter 3.

Next to carbon, silicon clusters have been studied widely. The first reported silicon clusters were generated by laser flash evaporation, quenched in a carrier gas and then cooled by supersonic expansion. Photofragmentation studies on mass selected silicon clusters were conducted. The reactivity of mass selected silicon clusters has been studied widely by using ion trap mass analyzers (Ref. 7).

Apart from carbon and silicon, other semiconductor elements such as germanium also form clusters. Both silicon and germanium also form nanoparticles, which are interesting today in view of their luminescence which can be tuned across a large window of wavelength. These are, however, investigated in the condensed phase.

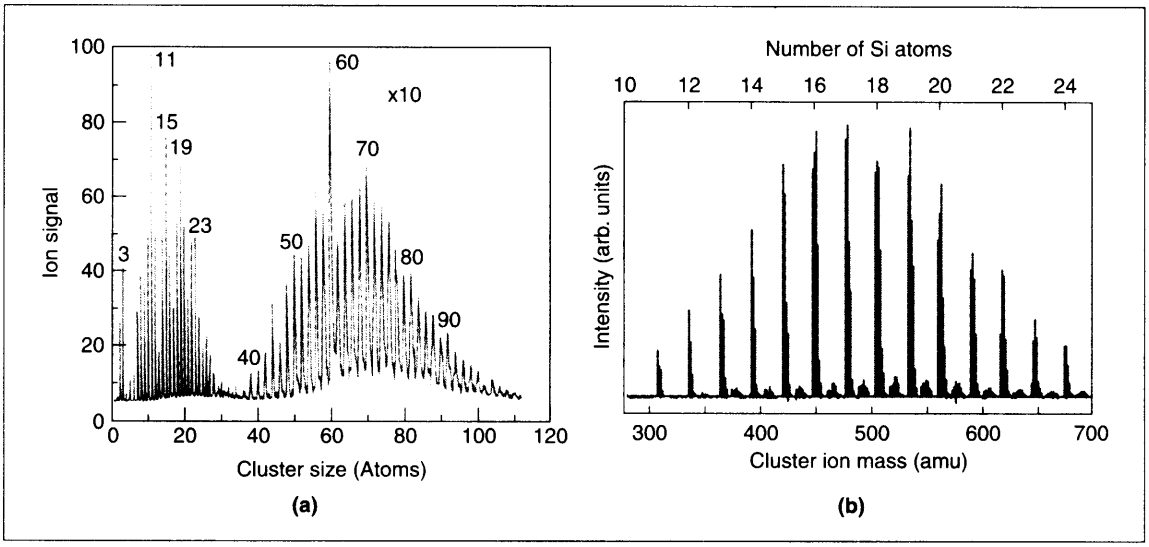

Fig. 6.7: *(a) Photoionization (PI)-TOF mass spectrum of carbon clusters. (b) Mass spectrum of silicon clusters. Reused with permission from, (a) E.A. Rohlfing, D.M. Cox, A. Kaldor. (1984) J. Chem. Phys., 81, 3322. Copyright 1984, American Institute of Physics. (b) S. Maruyama., M. Kohno, and S. Inoue. (1999) Thermal Science & Engineering, 7, 69.*

Apart from the bare metal clusters, metal oxides (e.g. MoO_3, WO_3, V_2O_5, FeO, LiO, MgO, PuO), metal chalcogenides (e.g. MoS_2, WS_2, TeS, FeS, ZnS, MoTe, Nb_2S_2, VS_4) and metal halides (e.g. $NiCl_2$, NaCl), are also known to produce clusters. The structural changeover from cyclic structure to the cage structure of MoO_3 clusters in gas phase has been reported recently (Ref. 8). A recent report shows the formation of magic number closed-cage clusters, from inorganic materials such as MoS_2 and WS_2 (Ref. 9). These negatively charged clusters, with the formula $Mo_{13}S_{25}$, are likely to be inorganic fullerenes with a cavity inside and may be formed by the curling of nanoflakes of MoS_2.

6.6.3 Metcars

These are closed-cage clusters made of metals and carbon. Various such clusters, such as Mo-C, Ti-C, Hf-C, V-C, Cr-C, etc. are known. Metcars were discovered by Castleman, *et al.* (Ref. 10) by laser vaporization of titanium metal in the presence of methane gas. The first cluster discovered had a stoichiometry, Ti_8C_{12}. This discovery has led a number of researchers to investigate analogues clusters. These clusters are called as 'metallocarbohedrenes' or met-cars. Photodissociation mass spectra of met-car ions show fragment ions with the loss of metal atoms. The chemical reactivity of met-car ions was found to be very high towards polar molecules like H_2O, NH_3, CH_3OH, etc. Several studies have been done on metcars, and the field has been reviewed recently (Ref. 11). Although the material is yet not synthesized in the laboratory as a bulk powder, the structure of the molecule is fairly well understood. This has a closed-cage as shown in Fig. 6.9 (Ref. 12).

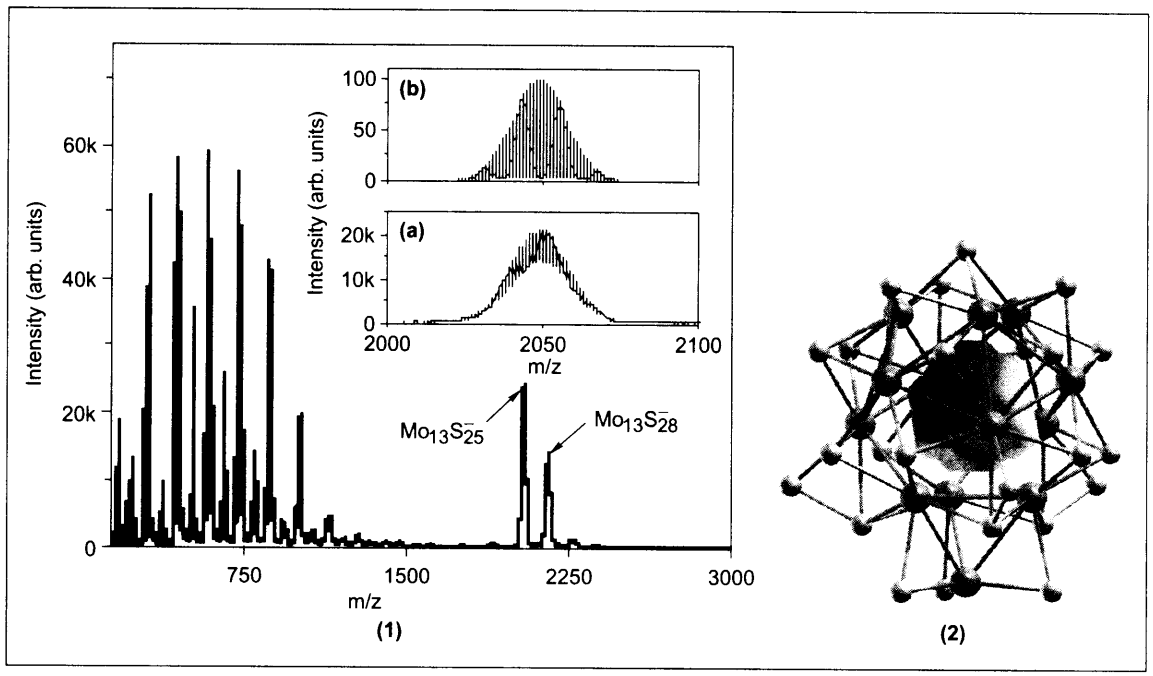

Fig. 6.8: *(1) Laser desorption ionization (LDI) mass spectrum of MoS_2 in the negative mode showing magic closed cage clusters. Inset: Experimental spectrum (a) shows the expected isotope distribution for $Mo_{13}S_{25}^-$ (b). (2) Atomic structure of the $Mo_{13}S_{25}$ cluster. A cloud in the center clearly showing the void space enclosed inside the cage-like structure of the $Mo_{13}S_{25}$ cluster. From the author's work, published in Ref. 9, Copyright (2005) American Chemical Society.*

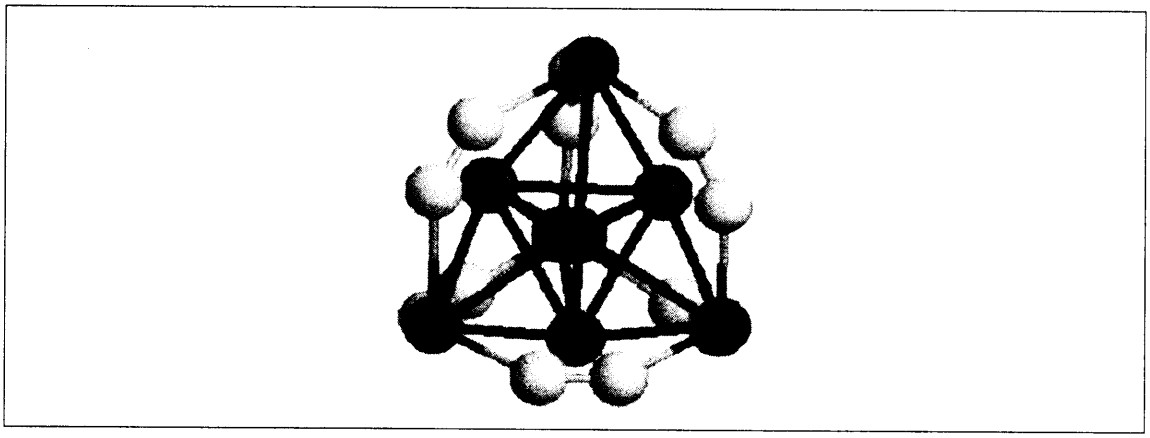

Fig. 6.9: *Optimized tetrahedral structure of the Ti_8C_{12} metcar. Titanium atoms are shown as dark and carbon atoms as light spheres. From Joswig, et al. (Ref. 12). Reproduced by permission of the PCCP Owner Societies.*

6.6.4 Rare Gas or Noble Gas Clusters and Magic Numbers

Rare gas clusters are the earliest clusters detected in molecular beam experiments. Detailed studies were carried out on these clusters as they were easy to make and their physical properties facilitated easy investigation. These rare gas elements have fully filled electronic configuration, as a result of which they are inert. Fig. 6.10 shows the mass spectra of positively charged Ar, Kr and Xe clusters (Ref. 13).

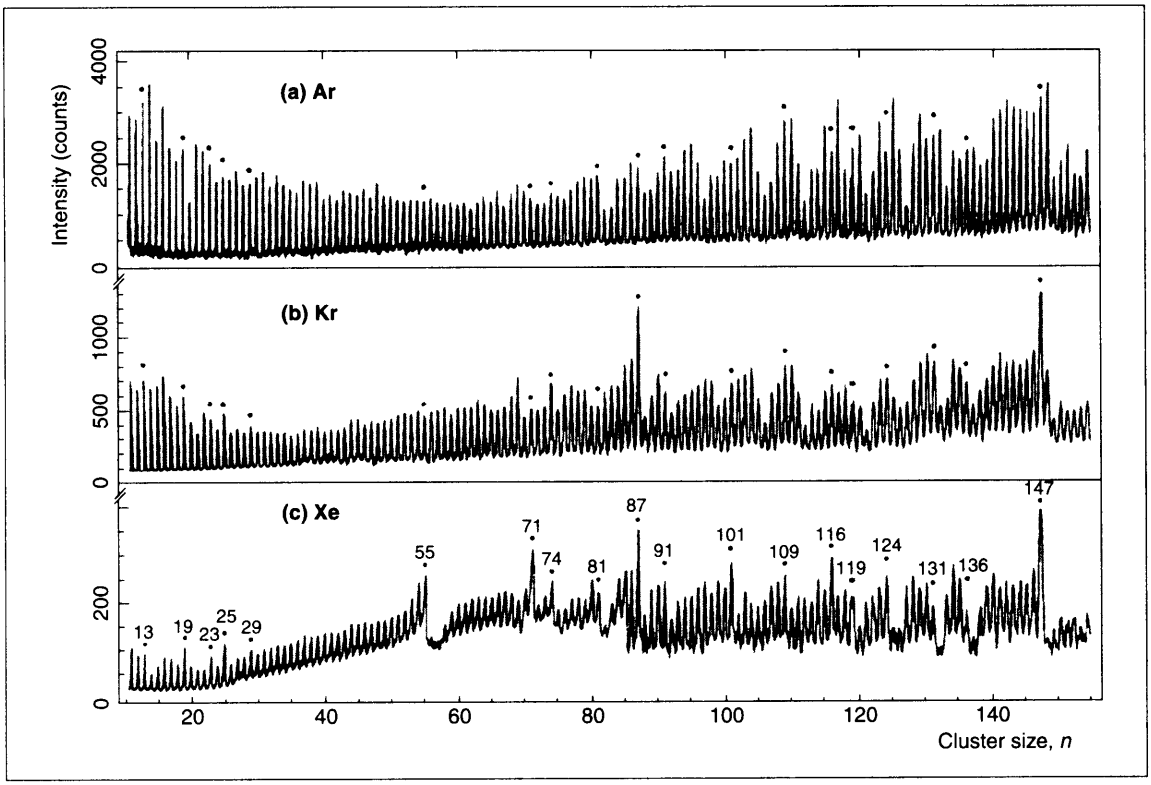

Fig. 6.10: *Mass spectra of positively charged Ar, Kr, Xe clusters. Reused with permission from, W. Miehle, O. Kandler, T. Leisner, and O. Echt. (1989) J. Chem. Phys., 91, 5940. Copyright 1989, American Institute of Physics.*

In the rare gas clusters spectrum, we see that a few cluster peaks have higher intensity than that of the nearer clusters. The nuclearities corresponding to those intense peaks are termed as magic numbers. The magic numbers in the mass spectra may arise due to the size-dependent binding energy of rare gas cations and the fragmentation processes that occur after ionization. The electronic structure of neutral rare gas clusters is different from that of the charged clusters. When we analyze the mass spectrum, the clusters with numbers N = 13, 19, 25, 55, 71, 87 and 147 are found to have high intense peaks. These magic-numbered clusters can be understood in terms of cluster structures consisting of polyhedral shells of atoms

around a central atom. For a geometric cluster composed of K icosahedral shells, the magic number of atoms is given by,

$$N(K) = 1 + \sum_{K=1}^{K} (10K^2 + 2)$$

Or, upon expansion,

$$N(K) = 1/3(10K^3 + 15K^2 + 11K + 3)$$

This equation explains the intense peaks at $N = 13$ ($K = 1$), $N = 55$ ($K = 2$) and $N = 147$ ($K = 3$), found in the mass spectrum (Fig. 6.10). The outer shells of these icosohedral clusters are known as Mackay icosohedra. These magic numbers are consistent with calculations on neutral rare gas clusters, using model interatomic potentials such as the Lennard-Jones potential, which predict a growth sequence based on maximizing the number of nearest neighbour contacts, so as to maximize the total cluster geometry.

6.6.5 Ionic Clusters

The term 'ionic clusters' signifies those clusters derived from ionic solids having large differences in electronegativity, such as NaCl, CsCl, etc. Ionic clusters may exist with positive or negative charge. Ionic clusters can be generated by methods like heating or laser vaporization of ionic compounds in a stream of cold inert gas. The studies on ionic clusters have made it possible to determine the size at which ionic clusters begin to acquire the properties of solids. Figure 6.11 depicts an example of ionic clusters from CsCl and CsI detected by mass spectrometry (Ref. 14). The size distribution is completely different in this case. Clusters with larger intensities correspond to the formation of structures similar to bulk solids.

6.7 Properties of Clusters

All properties vary with size, as all of them are dependent on energy. The energy of the system is affected by the fractional surface atoms and that makes properties change. It was proposed that the variation of physical and chemical properties can be predicted on the basis of cluster size equations (CSEs) (Ref. 15). These are of the form, $\chi(n) = \chi(\infty) + An^{-\beta}$ where χ is a property, which is a function of the number of atoms, n and A and β are constants ($0 \leq \beta \geq 1$). $\chi(\infty)$ corresponds to the bulk value. A variation of the properties can be given as in Fig. 6.12. In the cluster size regime, properties vary discontinuously while in the larger size regime, there is a smooth variation.

The properties of clusters explain the transition from single atoms to the solid state. This transition can be carefully examined with clusters. For example, one can ask the question when does a cluster of a metal indeed become a metal. One can systematically increase the cluster size and find out when specific features emerge in certain spectroscopic techniques. It is important to remember that such studies can also be done in the condensed phase with techniques such as STM.

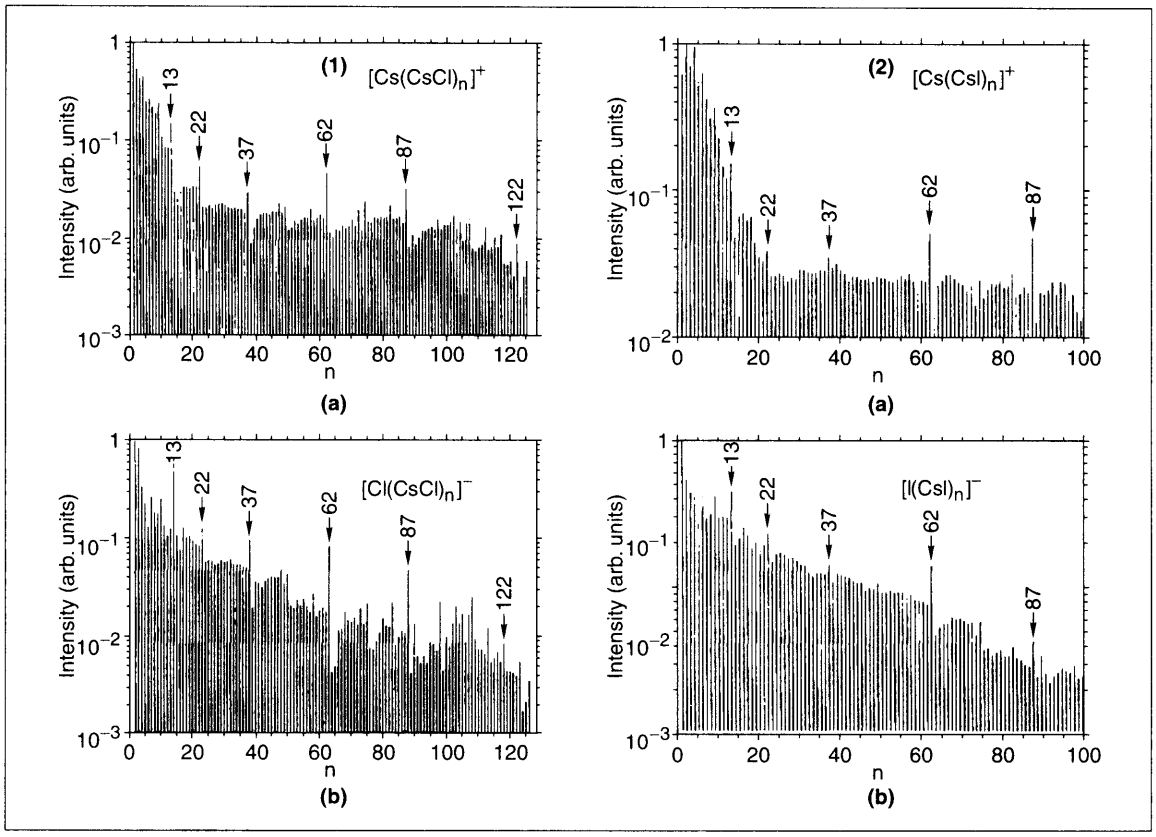

Fig. 6.11: *Mass spectra of (1) CsCl (2) CsI in (a) positive and (b) negative ion modes. Repninted with permission from, Y.J. Twu, C.W.S. Conover, Y.A. Yang, L.A. Bloomfield. (1990) Phys. Rev. B., 42, 5306. Copyright (1990) by the American Physical Society.*

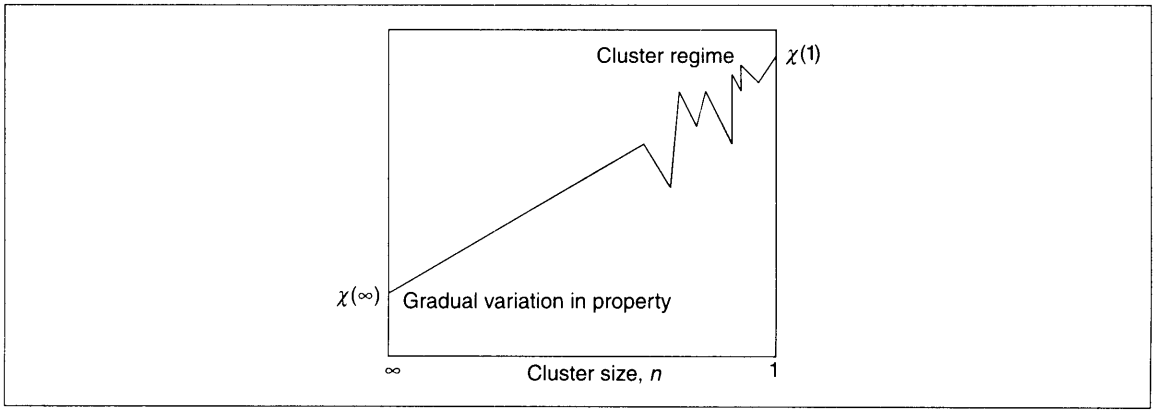

Fig. 6.12: *Variation in properties as predicted by cluster size equations.*

There are numerous properties which make clusters interesting. We will list a few examples. Mercury clusters show very interesting properties with respect to the size of clusters. They show a transition from van der Waals to metallic clusters (Ref. 16). We note that such changes are expected in a number of clusters but only a few are investigated in a large size range.

6.7.1 Mercury Clusters

The clusters are generated by a molecular cluster beam source. A typical mass spectrum of the clusters is shown in Fig. 6.13(a) (Ref. 16). A monochromatized radiation (typically from a synchrotron) is used to photoionize the neutral cluster beam. The light coming out from the undulator (one of the insertion devices in a synchrotron, used for enhanced light intensity) provides more than 10^{13} photons/sec/m rad. The photoionization efficiency (PIE) curve of each mass selected cluster ion is monitored by the variation

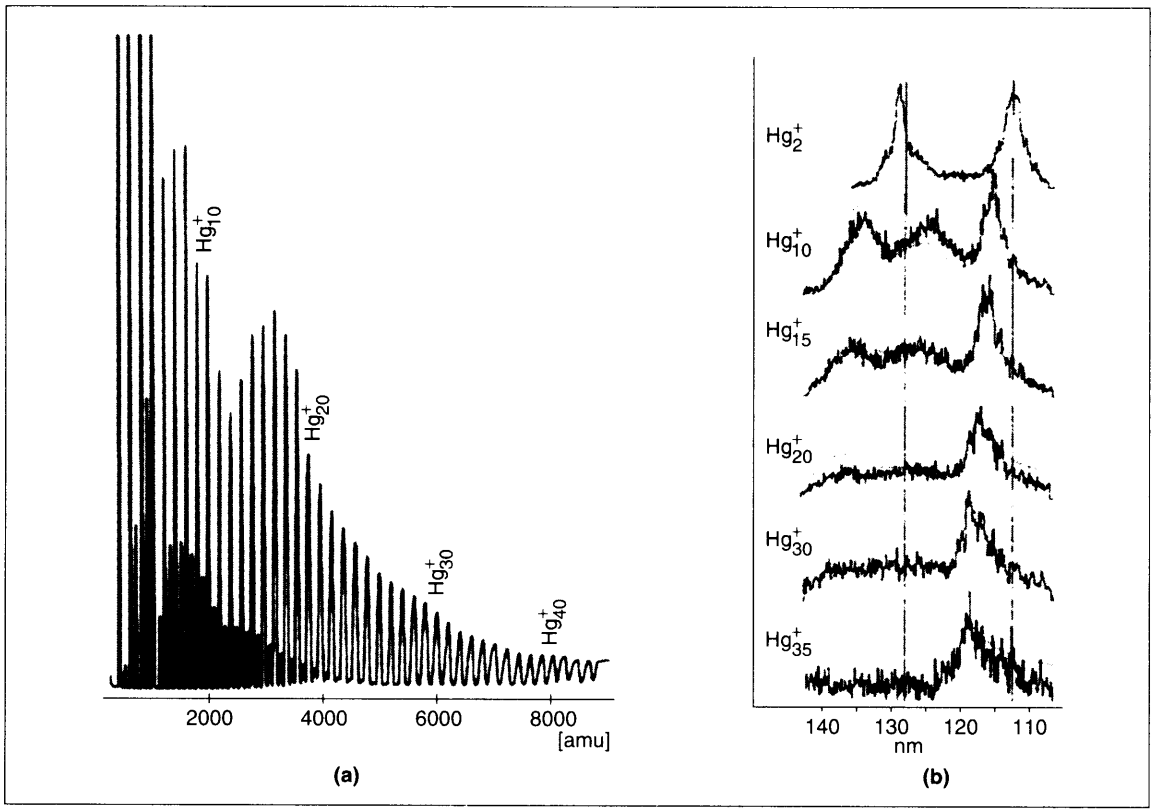

Fig. 6.13: *(a) Typical mass spectrum of mercury, obtained by electron impact ionization. (b) The recorded photoionization efficiency curves obtained for some mercury clusters. Reprinted with permission from, C. Bréchignac, M. Broyer, Ph. Cahuzac, G. Delacretaz, P. Labastie, J.P. Wolf, L. Wöste. (1988) Phys. Rev. Lett. 60, 275. Copyright (1988) by the American Physical Society.*

of the photon energy (Fig. 6.13(b)). The PIE curve of the atom is recorded between the ionization corresponding to the ejection of one *s* electron or one *d* electron. For small clusters with Hg_n ($n \leq 12$), the two autoionization lines are well resolved and appear to shift with respect to the corresponding atomic transition. For cluster size $n = 13$, the $1/n$ dependence is no longer observed in PIE. The gradually increasing shift for both lines illustrates the deviation from van der Waals bonding in larger cluster size (in which isolated atomic features are expected). In the size range $13 \leq n \leq 20$ the lines broaden significantly and their shifts show a deviation from the linear behavior. The spin-orbit splitting of the 5d levels increases with an increase in the cluster size. In the larger cluster size regime, $n > 20$, the spectral line shape is markedly asymmetric and is indicative of a transition from molecular to bulk metal-like properties.

6.7.2 Optical Properties

Optical properties of isolated clusters in the gas phase are rarely investigated. One can obtain information on the optical properties from photodetachment spectroscopy (technique by which electron removal of negatively charged species is investigated, see Chapter 2). From this one learns about the separation of energy levels of the neutral cluster and thereby get information on the optical absorption properties. It is also possible to do spectroscopy of isolated clusters (such as fluorescence) to obtain information on optical transitions. However, most of the optical studies are done in the condensed phase. For metals, the optical absorption gives beautiful colors, which has been the subject of investigation for a long time. In a metal cluster, in the metallic regime, there are free electrons which distribute throughout the cluster. As a result they are susceptible for external electric field. When a cluster is irradiated by light, which has a wavelength much larger than the cluster size, the electrical field is uniform as far as the cluster is concerned. The field induces collective oscillations of the electrons in the cluster. This aspect is discussed in greater detail in Chapter 9.

6.7.2 Ionization Potential

This is one of the well-studied properties of clusters. It was with this the shell structure and stability of clusters were confirmed. Ionization potential and electron affinity have been used to find the origin of metallicity in clusters (Ref. 17). At a critical size regime, the electron affinity of clusters become similar to the bulk. This has been investigated in metals such as copper and mercury. In the case of copper, metallicity was shown to appear in clusters as small as several hundreds of atoms. Origin of metallicity in mercury clusters has been investigated by photodetachment spectroscopy. By studying Hg_n^- ($n = 3$–250) clusters (Ref. 18), it has been shown that the *s-d* excitation band gap decreases with increase in size and by extrapolation, it was suggested that the band gap goes to zero at $n = 400 \pm 30$, when the cluster will behave like a metal. Such studies have been done on other transition metals too.

6.8 Bonding in Clusters

Here we discuss briefly two theoretical models, which are used to describe the structure and bonding of clusters. The structure varies between metallic clusters and noble gas clusters even though both have the same number of atoms. What is the reason for this kind of structural change? One can take for example the clusters formed from sodium and argon. Computations have been done to predict the structural and binding properties.

The comparison of these two types of clusters is interesting because their formation and binding are completely different. Delocalized electrons exist in a metal cluster. The situation is different in the case of noble gas clusters. All the noble gas atoms have a closed valence electron shell, as a result of which the valence electrons are localized near the ions, and the binding in these clusters arises due to van der Waals forces, which act between atoms in the cluster. With advances in computational capabilities many of the larger clusters are amenable for all-electron calculations. From such studies, total electronic structure and bonding of several clusters are now understood. The bonding in these systems is distinctly different from the traditional molecular systems. Often a specific valence state cannot be defined. For examples in the case of a 25 atom gold cluster stabilized by ligands, the valence state of the atoms involved in binding with ligand is not what we encounter in gold compounds. Similarly the metal-metal bonds are distinctly different from that of bulk gold.

Basically, two kinds of theoretical models are applicable for metallic clusters, of the type Na_n in order to predict their various properties. Properties like ionization potential and electron affinity vary with respect to the size of clusters. The two models are: 1) the Jellium model and 2) the liquid drop model. The Jellium model was originally developed to explain the structures and stability of atomic nuclei. This model was used to describe the electronic structure of the atom. The applicability of the Jellium model over a wide range from an atom to cluster makes it a major unifying concept. It is a quantum mechanical model with the quantization of electron energy levels arising due to the boundary conditions imposed by the potential. In this model, the metal cluster is considered as a uniform, positively charged sphere filled with electron gas. The Schrödinger equation is solved for an electron constrained to move within the cluster sphere under the influence of an attractive mean field potential due to the nuclei or ionic cores. This is in contrast to the classical Liquid Drop model, wherein there is no electronic structure. The solutions to the Schrodinger equation are the energy levels, $\psi_{n,l,m}(r, \theta, \phi) = R_{n,l}(r)Y_{lm}(\theta, \phi)$ and the energies (symbols have the same meaning as in the case of hydrogen atom). Therefore, the Jellium model gives rise to an electronic shell structure for clusters consisting of up to several thousands of atoms. The Jellium potential may be empirical, or alternatively *ab initio* effective potentials may be used. The potential may be modified for situations where spherical symmetry is not observed. Many of the predictions of this model have been verified with experiments, especially with alkali metal clusters.

A simpler model, the Liquid Drop model (LDM) has also been developed for metal clusters. This is an electrostatic model, in which the metal cluster is represented as a uniform conducting sphere. Variations of properties with size can be predicted by developing scaling laws using this model. According to the LDM, the IP should decrease as the cluster size gets larger (i.e. it requires less energy to remove an electron from a larger cluster than from a smaller one).

Review Questions

1. Are there specific properties we understood with the aid of clusters?
2. Why clusters are less stable in comparison to bulk materials?
3. Why do molecules form clusters?
4. Why clusters are generally investigated in vacuum?
5. Propose a method to make nanoparticles in bulk starting from gas phase clusters.
6. What are the important methods to make clusters in the gas phase?
7. Propose a study to understand a property of a bulk material using clusters not discussed in this volume.
8. Propose a method to make gas phase clusters, not discussed here.
9. Are there specific properties, other than those described here to study clusters?
10. List another way of classifying the various clusters, other than that described here.
11. What are the problems in making ternary clusters in the gas phase?

References

1. Boyle, R., (1661), *The Sceptical Chymist: or Chymico-Physical Doubts and Paradoxes*, London.
2. de Heer., W.A., (1993), *Rev. Mod. Phys.*, **65**, p. 611.
3. Bradbury, N.E., R.Nielsen, (1936), *A. Phys. Rev.*, **49**, p. 388.
4. Knight, W.D., K. Clemenger, W.A. de Heer, W.A. Saunders, M.Y. Chou and M.L. Cohen, (1984), *Phys. Rev. Lett.*, **52**, p. 2141.
5. Kéki, S., L. Szilágyi, J. Török, G. Deák and M. Zsuga, (2003), *J. Phys. Chem. B*, **107**, p. 4818.
6. Rohlfing, E.A., D.M. Cox, A. Kaldor, (1984), *J. Chem. Phys.*, **81**, p. 3322.
7. Maruyama, S., M. Kohno and S. Inoue, (1999), *Thermal Science & Engineering*, **7**, p. 69.
8. Singh, D.M.D.J., T. Pradeep, (2004), *Chem. Phys. Lett.*, **395**, p. 351.
9. Singh, D.M.D.J., T. Pradeep, J. Bhattacharjee, U.V. Waghmare, (2005), *J. Phys. Chem. A*, **109**, p. 7339.
10. Guo, B.C., K.P. Kerns, A.W. Castleman, Jr., (1992), *Science*, **255**, p. 1411.
11. Rohmer, M.M., M. Be´nard, J.M. Poblet, (2000), *Chem. Rev.*, **100**, p. 495.
12. Joswig, J.O., M. Springborg and G. Seifert, (2001), *Phys. Chem. Chem. Phys.*, **3**, p. 5130.
13. Miehle, W., O. Kandler, T. Leisner and O. Echt, (1989), *J. Chem. Phys.*, **91**, p. 5940.
14. Twu, Y.J., C.W.S. Conover, Y.A. Yang, L.A. Bloomfield, (1990), *Phys. Rev. B.*, **42**, p. 5306.

15. Jortner, J., *Z. Phys. D* (1992), **24**, p. 247.
16. Bréchignac, C., M. Broyer, Ph. Cahuzac, G. Delacretaz, P. Labastie, J.P. Wolf, L. Wöste, (1988), *Phys. Rev. Lett.*, **60**, p. 275.
17. Cheshnovsky, O., K.J. Taylor, J. Conceicao, R.E. Smalley, (1990), *Phys. Rev. Lett.*, **64**, p. 1785.
18. Busani, R., M. Folkers, O. Cheshnovsky, (1998), *Phys. Rev. Lett.*, **81**, p. 3836.

Additional Reading

1. Roy L. Johnston, *Atomic and Molecular Clusters*, Taylor and Francis, London (2002).
2. Boris M. Smirnov, *Clusters and Small Particles in Gases and Plasmas*, Springer-Verlag, New York (2000).
3. Paul–Gerhard Reinhard, Eric Suraud, *Introduction to Cluster Dynamics*, Wiley–VCH Verlag GmbH & Co. KGaA, Weinheim (2004).
4. Faraci, G. and P. Selvam in *Encyclopedia of Nanoscience and Nanotechnology*, Edited by H.S. Nalwa, American Scientific Publishers (2004).

Chapter 7

Semiconductor Quantum Dots

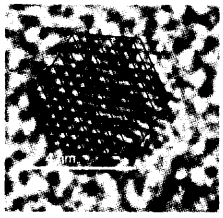

Quantum dots are the very first extensively researched nanoparticle systems. We learned many of the properties of electronically confined systems through such investigations. Their optical, photophysical, photochemical, biological and catalytic properties have opened up numerous application possibilities. Several of these have been realized such as the dye sensitized solar cells which utilize the electronic properties of these materials. The applications in biology using these materials are some of the most extensively researched areas in nanobiology, covered separately in this book. In this chapter we look at the reasons for the unique properties of nanocrystals, their synthesis, experimental investigations and applications.

Learning Objectives

- What are quantum dots?
- What is quantum confinement?
- How can one make and study quantum dots?
- What properties of quantum dots have been discovered?
- What are their applications?

7.1 Introduction

Semiconductor quantum dots signify a class of materials in which quantum confinement effects are investigated in greater detail. They are also referred to as 'semiconductor nanocrystals'. In fact these constitute a sub-class of a broad family of nanoparticles, which include semiconductor, metal, insulator, organic, etc. particles. 'Quantum dots' is a term referred only to semiconductor particles, while 'nanocrystal' can be any inorganic entity in which there is a crystalline arrangement of constituent atoms/ions. In a macroscopic semiconductor crystal, the energy levels form bands. The valence band is filled and the conduction band is completely empty at 0 K. The bands are separated with a specific energy gap, E_g. When an electron gets excited due to thermal excitations, an electron–hole pair is created. The electron in the conduction band and the hole in the valence band can be bound when they approach each other at a finite distance. This

bound pair is called an 'exciton', which is delocalized throughout the crystal. The Bohr radius of the exciton can be given as: $a = h^2\varepsilon/4\pi^2e^2[1/m_e + 1/m_h]$, where ε is the dielectric constant of the material, m_e and m_h are the effective masses of electron and hole, respectively, and e is the elementary charge. Quantum size effects are manifested when the length of the nanocrystal made, d, is comparable to the exciton radius, a. This is ~ 56 Å for CdSe. Note that the unit cell dimensions of the semiconductor are much smaller than the characteristic length. The de Broglie wavelength in materials, $\lambda = h/mv$, is in the range of nanometers and strong confinement effects are manifested only when the particle dimension approaches this value. At this dimension, most materials have structures similar to those of their bulk counterparts, at least in the core of the particle.

The electronic structure of materials is strongly related to the nature of the material. In a three-dimensional object of large size, the electronic structure is not restricted by the dimension of the material. The wavelength of electrons is much smaller than the typical length of the material. When the electronic motion is confined in one dimension, and it is free in the other two dimensions, it results in the creation of 'quantum wells' or 'quantum films'. The quantum well notation implies that the electrons feel a potential well as they are trapped in the film. The quantum film notation is self-explanatory. Here the density of states shows a step-like behaviour. In the case of a one-dimensional system, i.e. when the electrons are free to move only in one direction, we get a situation wherein the density of states shows a Lorenzian line shape. Such a situation can be seen in carbon nanotubes. If the electrons are confined to a point, we get a zero-dimensional system, wherein the electrons are not free to move at all. Here we get states which are molecular in nature. The situation is schematically depicted in Fig. 7.1. What is shown in Fig. 7.1 is that while the density of states is smoothly varying in bulk materials, it shows discontinuities in confined systems. This will lead to steps in two-dimensional confinement, singularities in one-dimensional confinement and discrete lines in zero-dimensional confinement.

Some of the properties which change drastically as a function of size are the optical properties, including both the absorption and emission of light, which is evident from Fig. 7.1. Nanocrystals have discrete orbitals. The energy of the first level will be shifted from the position of the bulk value by $h^2/8m_ea^2$ where a is the diameter of the particle. Remember that the particle in a box model predicts the energies of the levels as, $n^2h^2/8m_ea^2$ ($n = 1, 2, \ldots$). The simplest model of a quantum dot would be a particle in a sphere model, assuming that the nanocrystal is a sphere. This does not make a difference in the energy level description mentioned above. The energy gap increases with a decrease in a. As a consequence of this, the CdSe nanocrystals emit light anywhere from 4500 to 6500 Å, so that any color from blue to red is achievable, depending on the size of the particle.

It may be worthwhile to describe the issue of confinement again. These particles are called quantum *dots* as their electrons are *confined* to a point in space. They have no freedom in any dimension and electrons are said to be localized at a point, implying that a change in all directions changes the properties (in reality, a dot is a three-dimensional object comprising several hundreds or thousands of atoms, with finite shape). Compare this tiny unit of matter with semiconductor structures which are grown by thin film evaporation methods, which facilitate the creation of ultra thin films wherein the thickness is comparable to a, the diameter mentioned above. Such a material is called a 'quantum well', implying that the electron is confined within a two-dimensional area, which is said to be a 2D confinement. It is important to recall that the well itself is made by evaporation and the material of interest is confined inside another material

of larger dielectric constant. Confinement along one direction results in a quantum wire, leaving the electron free to move only along one direction. This is known as a 1D confinement. In the quantum dot, there is no freedom along any direction.

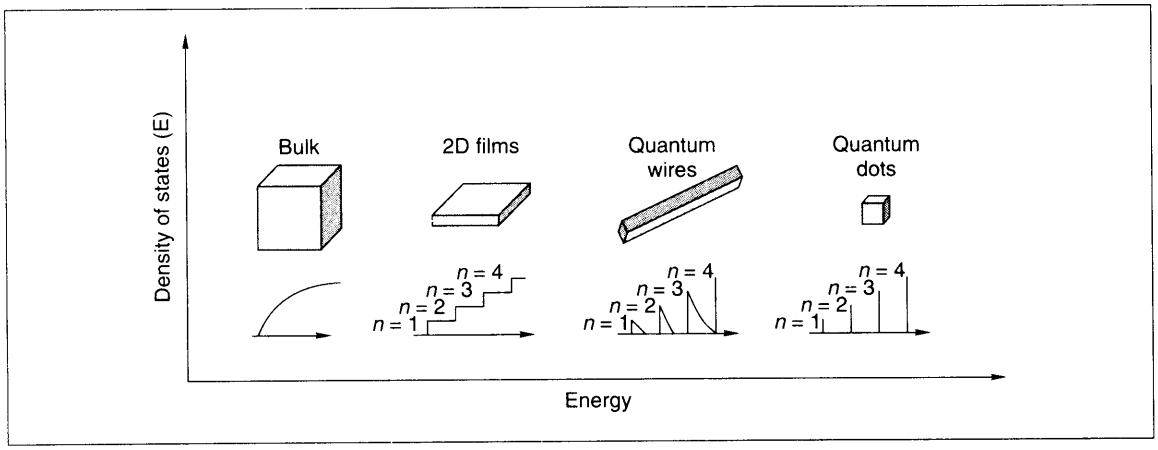

Fig. 7.1: *Quantization of the electronic density of states as a result of variation in the dimensionality of materials.*

An ideal quantum dot is realizable only when the electronic states within the dot face a discontinuity at the edge of the material. Due to this, the electron within the dot feels an insurmountable barrier at the edge. When a material is truncated at the surface, the surface atoms have unsatisfied valencies. In order to reduce the surface energy, the surface reconstructs, which leads to energy levels in the forbidden gap of the semiconductor. The electrical and optical properties of the material are degraded by these traps. In an ideal semiconductor nanocrystal, the surface atoms are bonded to other materials in such a way as to remove the defects. This is what is done when a dot is covered with a material of larger band gap. In an ideal quantum dot, when there are no defect sites for charges to get trapped, the quantum yield of luminescence will be very high, nearly one. The emission will also be sharp. Better light emission occurs as the electrons and holes are confined spatially. This is achieved by chemically protecting the surface with proper protecting molecules called 'capping agents'. Since the surface of the nanocrystal can be modified by using various capping molecules, these materials can be adapted to suitable media, including biology. They are therefore ideal probes in a biological environment.

An important aspect of nanocrystals (NCs) is that they link molecules and bulk materials. The properties change continuously as a function of size in the regime of NCs. Thus if the diameter is changed from 11.5 nm to 1.2 nm, the band gap of CdSe NCs can be changed from 1.8 eV to 3 eV. This corresponds to light emission from red to blue. The size regime of nanocrystals is difficult to pinpoint and depends on the material. In the case of most materials, it lies in the range of 100 to 1,00,000 atoms. The lowest size regime arises because at this point the structure changes to that of molecules (and consequently the properties). In the larger size regime, the system is nearly bulk-like as its energy level spacing is comparable to that of thermal energy.

7.2 Synthesis of Quantum Dots (QDs)

The kind of method used for the synthesis of quantum dots depends on the properties. Ideally, nanocrystals should have the following properties:

1. Monodispersity
2. Possibility of further chemical derivatization
3. High degree of crystallinity and specificity (avoiding polymorphic phases)
4. Chemical integrity
5. Lack of defects

There are several methods in literature for the chemical synthesis of nanocrystals. All of them can be grouped under certain broad classes. It may be noted that there are also other approaches such as 'biological synthesis', which has been receiving some attention recently (Ref. 1).

7.2.1 General Strategies

In the synthetic protocol, two kinds of general approaches are used, the top-down approach and the bottom-up approach. In the top-down method, the bulk material is brought into a smaller dimension by various tools. Numerous methods are included in this category such as the various tools of patterning used to make structures in semiconductor electronics. These include chemical etching, optical lithography, use of particle beams (such as electron, ion and atom), etc. Apart from these, various methods are used to create ultra thin films of the material under investigation. These include thin film evaporation, molecular beam epitaxy, etc. These tools will not be discussed in the context of nanomaterials as it is difficult to obtain large quantities of materials by using them. However, there are other methods of creating powders starting from bulk materials. These techniques utilize various methods of milling and grinding, of which ball milling is the most commonly used one.

In the bottom-up approach, one can use gas phase or liquid state approaches. In the gas phase approach, the material to be synthesized is mixed in the atomic state in the gas phase itself. For this, the atoms of the materials are produced *in-situ* in an evaporation apparatus. This may also involve reacting atoms of one element with a gas phase species (such as oxygen). The prepared material in the gas phase is condensed to get the bulk material. At the stage of condensation, stabilizers may be added. Monodisperse metal particles are made in this way. Bulk powders of several oxides can be conveniently made by this route. This methodology may also be referred to as top-down as the synthesis starts from the bulk materials, which are subsequently evaporated.

The principal synthetic strategy used to make nanoparticles in a solution can be classified as 'arrested precipitation'. Here at some stage of the growth of the particles, the surface is stabilized and further growth is arrested. This is commonly done by surfactants which bind to the surface of the growing nanocrystal. This synthetic approach, which is used for various kinds of materials, is similar to that used for

metal nanoparticles. Various kinds of surfactants, both ionic and covalent, have been used for this purpose. Arresting of the growth can be achieved in cavities such as those of micelles, zeolites, membranes, etc. Arresting can also be brought about by sudden variation in temperature and pressure conditions leading to quenching.

All the nanoparticles formed are stabilized in the solution by the presence of an electrical double layer when the protecting agents present are ionic in nature. This is typically seen in the case of metal nanoparticles such as gold when the reduction is done with sodium citrate. The surface of the nanoparticle is protected with anions and cations. In the specific case mentioned, the anions are citrate and chloride, while the cations are sodium and protons (as gold is completely reduced). The electrical potential created by the double layer is large so that Coulomb repulsion prevents aggregation. On closer contact between the particles, the interaction potential rises sharply due to charge repulsion. However, there is van der Waals attraction at larger distances and the net result is that there is a weak potential minimum at a moderate distance. This stabilizes the nanoparticle dispersion. These dispersions cannot be concentrated beyond a point as the particles agglomerate. However, in dilute solutions, many colloidal solutions are stable for extended periods, such as in the case of gold. If they are precipitated, metallic mirrors are obtained. In the case of semiconductor materials, the bulk material is formed. However, it is possible to change the surface cover to a covalent one and achieve subsequent purification. In the case of covalently bound ligands, there is no net charge and the particle behaves like a molecule. These materials can be precipitated, re-dispersed and stored for extended periods.

Some of the techniques used for synthesis are discussed in more detail in the following sections.

7.2.2 Synthesis in Confined Media

In this approach, nanoparticles are synthesized in a space that is already available. The chemical reaction occurs inside a reactor, which is prepared by one of the several ways. Among the various confined media, reverse micelles, Langmuir–Blodgett films, zeolites, porous membranes, clays, etc. are worth mentioning. They all have spaces of the order of nanometers, in which ions can be put. A proper stoicheometric mixture can be provided and the reaction conditions can be altered to produce the required nanocrystal. The chemistry in the solution phase can be conditioned to allow the usage of proper molecules for surface passivation.

For example, one can conduct the reaction in reverse micelles (water in oil). Here oil is the majority phase while water is the minority phase, and nanoscopic containers are formed by micelles. One can add metal ions and organometallic reagents into the nanoreactors, leading to the following reaction:

$$CdCl_2 + Se(SiMe_3)_2 \rightarrow CdSe + 2Me_3SiCl$$

The medium can have capping agents as a result of which the surface prepared is passivated. The oil/water ratio and the temperature conditions can be adjusted to obtain suitable particle dimensions. The materials can be separated from the solvent system and further annealed by heating in a higher boiling solvent to improve the crystallinity.

In confined cages such as those of zeolites, the maximum dimension of the particle formed is fixed. In a typical approach, the exchangeable ions such as Na^+ in the zeolite are exchanged with Cd^{2+} by washing the zeolite with a Cd^{2+} solution. The sample is then exposed to H_2S. Depending on the extent of Cd^{2+} present in the sample, various nanoparticle sizes are obtained. The same method can be used in membranes such as Nafion® which have empty spaces of the order of nanometers.

7.2.3 Molecular Precursors

In the precursor route, nanorystal seeds are prepared in a medium which can control the growth of the particles by co-ordinating with it. The solvent universally chosen for this approach is trioctylphosphine oxide (TOPO), which has high thermal stability and can co-ordinate with inorganic surfaces. The co-ordinating TOPO can be exchanged with other ligands after isolation. The nanocrystals prepared this way can undergo Ostwald ripening (growth of larger particles at the expense of smaller ones) as a result of which monodisperse particles can be formed. A number of materials have been prepared by using the TOPO route. In a standard method, the metal ion precursors are added into hot TOPO while stirring continuously (an injection of the ion precursors is made into a hot solution, as seen in Fig. 7.2). The difficulty of using pyrophoric compounds at elevated temperatures constitutes a risk and to avoid this, a single compound delivering both the constituent elements in the semiconductor has been developed. Cadmium dithiocarbomates (e.g. $Cd(S_2CNEt_2)_2$) can produce CdS nanocrystals. A variation of chemicals can get other semiconductors. The synthetic protocol can be modified by changing the solvent (using a mixture of surfactants instead of TOPO), synthesis parameters such as volume and the number of injections, etc. These modifications have resulted in the formation of various morphologies, apart from the common spherical particles. It may be n ted that even the spherical particles are faceted.

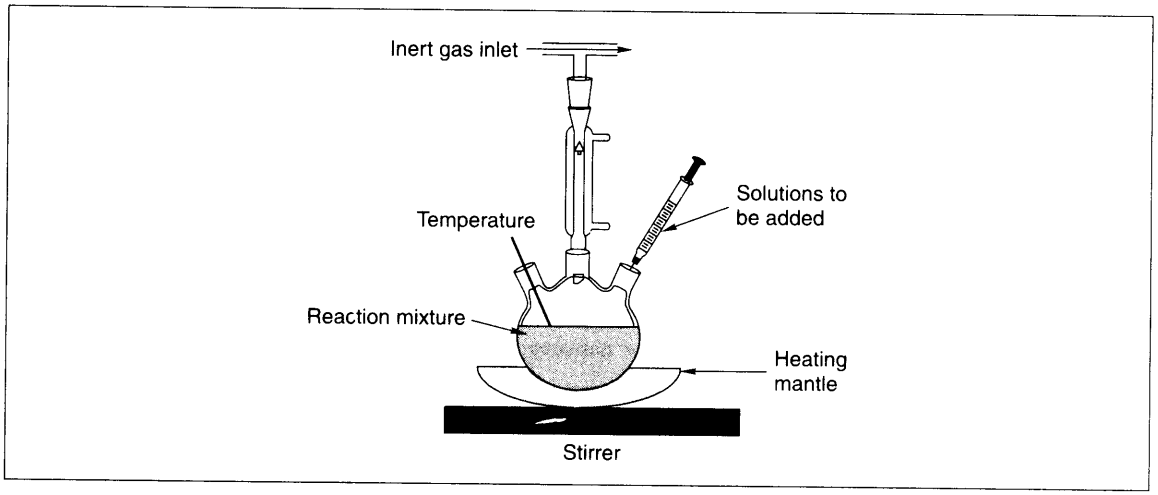

Fig. 7.2: *Typical chemical synthesis approach for making nanoparticles, especially QDs. These are made at higher temperatures, produced by a heating mantle. The process is carried out in an inert atmosphere. Solutions may be added simultaneously.*

7.2.4 Chemical Synthesis Using Clusters

Nanocrystals are large molecules. Therefore, it is natural to think of building them starting from atoms. This atomic building approach has many advantages, one of which is the removal of all possible defects while the other is the possibility to have truly monodisperse materials. A larger cluster can be constructed from a smaller one. Using a starting cluster compound, $[(NMe_4)_4Cd_{10}S_4(SC_6H_5)_{16}]$ the cluster, $Cd_{32}S_{14}(SC_6H_5)_{24}$.4DMF has been prepared (Ref. 2). This is a cluster with a well-defined structure similar to the structure of bulk CdS. The absorption spectrum of the cluster is blue shifted in comparison to the bulk CdS (358 nm). More complex structures have been built by using this approach.

It is important to consider the crystalline state of the nanocrystal while deciding its properties. The effective masses of electrons and holes depend on the crystal structure of the material, as a result of which all the optical, photophysical and photocatalytic properties will be affected by the structure. In the case of CdS and ZnS, there are two distinct crystalline forms, cubic (zincblende) and hexagonal (wurtzite) structures. CdS exists in the bulk in the wurtzite form while ZnS is found in the cubic form. When synthesized, CdS mostly adopts the cubic form, which is metastable. However, hexagonal CdS can be synthesized in the nano form. By controlling the surface functionalization, ZnS has been made in different forms. When protected with compounds such as 1-hexanethiol, 1-decanethiol, benzoic acid, etc., ZnS nanocrystals exist in the cubic form, while in the unprotected case, they exist in the hexagonal form. When the surface of the nanocrystal is not bound to the interacting molecules, one gets the metastable hexagonal phase. Thus it appears that surface stabilization leads to the formation of the cubic phase. Obviously, surface energy plays a significant role, as the reduction in surface energy by surface stabilization leads to the formation of the stable phase. It is important to note that the energy difference between the cubic and hexagonal phases is small (3.2 kcal mol^{-1}), which facilitates transformation.

Current wet chemical methodologies can give highly monodisperse particles. High monodispersity implies a distribution of less than 5 per cent in the particle dimensions. The typical capping agent is TOPO or trioctylphosphine selenide (TOPSe), in the case of CdS and CdSe particles, respectively. These groups bind to the surface Cd atoms and the coverage changes, depending on the size of the particle. While almost all the surface Cd atoms are protected in a smaller crystallite, only half of them are covered in the case of a flat surface. This is because as the size decreases, the surface area increases and molecules get adequate space to arrange themselves.

7.2.5 Modification of the Surface of Nanocrystals

The surface modification of nanocrystals is important for the following reasons:

1. It removes surface states, thus making near band gap emission possible. Due to the removal of defects, the emission becomes narrow.
2. It adds chemical versatility to the system allowing it to become part of a larger structure. This is important in the use of such materials in polymers, inorganic matrices, etc. It is also important in making the system biocompatible.

3. Surface passivation and suitable functionalization make the system chemically inert and thermally stable. In fact, various attributes can be added to the nanocrystal by appropriate modification. This includes chemical and biological compatibility, hydrophobicity, hydrophylicity, etc.

The most common approach used is that of functionalizing the surface of the nanocrystal with various molecules, which can be thiols, amines, alkyl or silyl groups, etc. In all these cases, the chemical functionality of the molecule interacts with the metal atom at the surface of the nanocrystal. The other approach involves the functionalization of the molecule further. For example, aminopropyltriethoxysilane coupling agent can be used to functionalize the surface of the nanocrystal. The surface will have ethoxy groups which can be hydrolyzed. By using a silica forming precursor, one can form a silica shell around the nanocrystal. The coating of CdS with a thin layer of HgS and further with CdS-yielding CdS/HgS/CdS structures, has also been reported. This structure would be called a 'quantum dot–quantum well' structure in the sense that a quantum dot is covered with a two-dimensional structure with a large dielectric barrier. This construction becomes possible as cubic CdS has a lattice constant similar to that of cubic HgS.

One of the important advantages of such a shell structure is the retardation of charge recombination in semiconductors upon photoexcitation. The electron that is created in the large band gap material upon photoexcitation can be stabilized in the lower lying conduction band of the other material. The direction of electron flow can be controlled in this fashion and a rectifying action has been observed (Ref. 3).

7.2.6 InP Nanoparticles

As an example of the preparation of semiconductor nanocrystals, we will discuss the protocol used for InP quantum dots. This is called a group III–V semiconductor as In belongs to group III and phosphorus to group V. The indium precursor used is indium oxalate, indium chloride or indium fluoride. Trimethylsilylphosphine is used as the phosphorus precursor. A mixture of TOPO and trioctyl phosphine (TOP) is used as the colloidal stabilizer. The precursor species are mixed in an atomic ratio of 1:1 to make an InP precursor in the presence of the colloidal stabilizer. TOP is used in a ratio that is ten times larger than that of TOPO. The mixed solution which forms the transparent precursor is heated at 250–300 °C for three days to obtain the colloidal solution. Depending on the size range desired and the extent of crystallinity, the dispersion can be heated to varying time/temperature. The decomposition temperature of the precursor is >200 °C. The particle size can be modified by controlling the rate of decomposition. The material synthesized has a monolayer cover of TOPO/TOP. This makes the material disperse in a hexane:butabol mixture (0.9:0.1 by volume) containing 1 per cent TOPO. Precipitation of the nanocrystals can be achieved by adding methanol to the dispersion. This process is repeated. Dispersion and precipitation are carried out to remove unreacted materials or other products. TOPO is added as repeated washing can remove it from the surface of the nanocrystal and thereby affect colloidal stability. The protective cover can be replaced with thiols, amines, fatty acids, sulfonic acids, polymers, etc. It is also possible to bind the surface with proteins. Almost any functionality can be added by suitable chemistry. The material thus prepared can be precipitated, purified and redispersed as in the case of metal nanoparticles. Depending upon the functionality they will be dispersable in appropriate solvents; polar or non-polar. The polarity of

the solution can be changed gradually. This approach helps precipitate particles gradually. The narrower the distribution of the parent material, the narrower are the precipitated particles as well.

The preparation method can get *n*-doped, *p*-doped and undoped particles. *N*-doping is achieved by the addition of S, while *p*–doping is done by adding Zn. These are done by mixing suitable precursors to the InP precursor-forming solution. Such InP:S and InP:Zn nanoparticles are also stable.

7.3 Electronic Structure of Nanocrystals

The electronic structure of complex systems can be understood on the basis of simpler systems. For example, graphite can be understood starting from an assembly of benzene fragments, or diamond can be thought of as an assembly of tetrahedrally connected sp^3 carbon atoms. Benzene has discrete π and $\pi^\star$ states. As the number of rings increases, the highest occupied molecular orbital moves up in energy while the lowest unoccupied orbital moves down in energy. As a result, the energy of the transition decreases. This can be seen from ethylene to polyenes and from benzene to pentacene. The energy difference between the π and $\pi^\star$ levels decreases and eventually it becomes smaller than thermal energy. At this stage, the levels are considered to be merged to form bands. In the case of an infinite ring containing solid, as in the case of a single sheet of graphite, the gap reduces to zero and the top of the valence band (the HOMO) touches the bottom of the conduction band (LUMO). This makes it a semimetal. Other similar situations may be envisaged in the kind of infinite chains such as polyenes and polyynes. When the gap cannot reduce to zero, we obtain situations categorized as semiconductors or insulators. The reduction in the energy gap with an increase in the number of electrons is illustrated in Fig. 7.3.

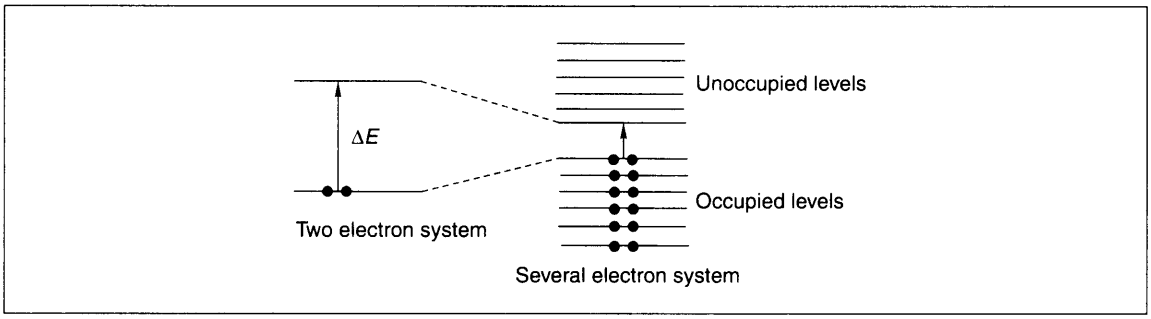

Fig. 7.3: *The change in the electronic energy levels of the system when the number of structural units increases, as in the case of a change from one double bond to many double bonds. The energy gap between the levels, corresponding to the first excitation energy, ΔE decreases. When the number of double bonds increases significantly, the energy levels merge and the gap becomes comparable to that of thermal energy.*

This discussion obviously implies that a material will behave differently when the size regime is smaller than that required for bulk properties. Although this discussion was in the context of electronic

properties, every other property will change as most of them are electronic in origin. This variation makes the question, 'At what size do properties become bulk-like', valid. This depends on the material of choice. In the case of elements such as carbon, with the smaller size regime containing a few tens to hundreds of carbon atoms, we have molecules called fullerenes. Their electronic structure is similar to that of the molecules which we are familiar with. Even in the regime of hundreds of atoms, their bonding and several other properties bear close similarity with those of bulk materials such as graphite. This is true of many elements. In the case of silicon, smaller clusters are entirely different and a bulk-like structure is exhibited only in the larger size regime of 10^3 atoms. Although the lattice constants may be similar to bulk, the electronic properties may not reach the bulk limit. In a few cases, this bulk-to-molecular changeover has been investigated and has been discussed in Chapter 6 on gas phase clusters.

The above discussion suggests that the bulk band gap increases with a decrease in the size of the material. Electronic transitions across the band gap result in the spectroscopic properties of the system. The variation in absorption edge can be seen as a function of the particle size. This aspect has been investigated in detail. In addition to the states which are created outside the band gap, in a real nanocrystal, there are also states within the band gap, which are created as a result of defects. It is possible to calculate the diameter of the nanoparticle from the position of the absorption edge. The nanocrystal can be considered as a three-dimensional box and the energy gap can be related to the diameter of the particle or the width of the well.

While dealing with nanocrystals, one has to distinguish between three different kinds of size regimes. Various effects in these size regimes have been the subject of investigation, but we will not discuss this in great detail. The size regimes depend on the nanocrystal radius, r and the bulk exciton radius, a. In the strong confinement regime, $r \ll a$, the Coulombic interaction between the electron and the hole is much smaller than the confinement energies, and therefore, electron and hole can be considered as separate particles. A weak confinement regime, $r \gg a$, occurs when the electron and hole motions are strongly correlated, as electron–hole interactions are significant in comparison to the confinement energies. In the intermediate regime, $r \sim a$, the electronic structure depends strongly on both quantum confinement and Coulomb interaction.

The simplest model used to represent the energy states of a nanocrystal is a spherical quantum well, with an infinite potential barrier. Although the model is simple, if we include the Coulombic interaction between the electron and the hole, analytical solutions for the Schrödinger equation will not be possible. Disregarding the e-h interaction is possible in the strong confinement regime, as confinement energies scale with d^{-2} (as energy goes as n^2/d^2) while Coulomb interaction scales with d^{-1}. This results in states with distinct n, l, m quantum numbers referring to various symmetry, orbital angular momentum, its projection, respectively (similar to electrons in orbitals of an atom). The wave functions are represented as products of several terms. The energies of the states can be given as:

$$E_{l,n}^{e,h} = h^2 n^2 / 8\pi^2 m_{e,h} d^2$$

where n is a quantum number. The exact nature of the wave function and the quantum number are not introduced here. The wave functions correspond to the S, P, D, ..., etc. states depending on the orbital angular momentum, l. There is one more quantum number, m which decides the degeneracy of the states. A pictorial representation of the energy states is given in Fig. 7.4. The energies are measured from the

bottom of the conduction (valence) band for electrons (holes). The energy increases as one goes higher in the quantum number. Since the electron mass is much smaller than that of the hole ($m_h/m_e \sim 6$ in CdSe), the electron levels are separated more widely than the hole levels.

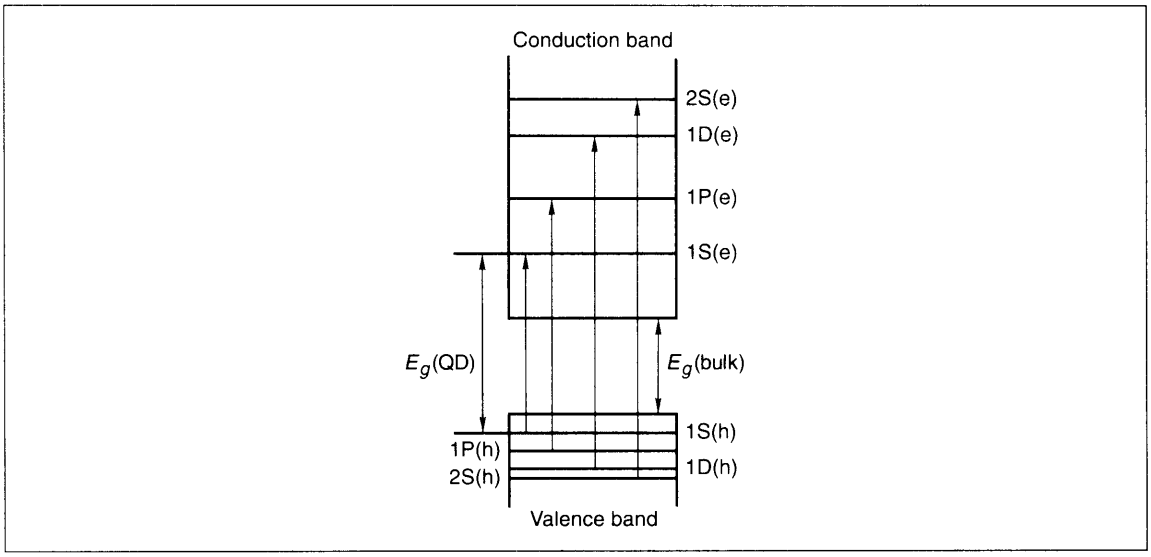

Fig. 7.4: *The electronic states of a nanocrystal. The allowed optical transitions are marked.*

Electronic transitions are possible between various energy levels. However, the wave functions corresponding to different n and/or l are orthogonal and therefore it is not possible to observe all these transitions. Optical transitions between states of the same symmetry can, however, be observed. The intensity of the transition will be related to the degeneracy of the states in question. The transitions observed are far more complex than those described by the spherical quantum well model. The description given here is inadequate to describe the hole states. Spin-orbit and Coulomb e–h interactions have to be considered to improve the energy level picture.

One of the important aspects to be considered while interpreting experimental spectra is the size range of particles prepared in a typical synthesis. Spectroscopic size selection can be done by using techniques such as fluorescence line narrowing (FLN), spectral hole burning and photoluminescence excitation (PLE). In these techniques, a narrow energy window is used for excitation (first two) or detection (last). This makes the technique sensitive only to a specific particle size. Size selection with the red region of the spectrum is preferable as it helps select the particles of the largest size in the ensemble.

7.4 How Do We Study Quantum Dots?

A quantum dot material prepared by one of the methods described before will be a powder. One needs to characterize its physical, structural, electronic and other properties to qualify it as a nanomaterial.

Several of the tools outlined in the earlier chapters may be used in this regard. We shall illustrate the most essential aspects of the characterization of quantum dots through the use of some of the tools. Several other tools may also be used for additional information. These methods may be used for any nanomaterial, irrespective of their nature.

7.4.1 Absorption and Emission Spectroscopy

Absorption and emission spectroscopy are performed to understand the quantum confinement of the system. The spectra are measured in absorption and fluorescence spectrometers for absorption and emission, respectively. For these measurements, one typically uses a solution in an appropriate solvent which does not have characteristic absorption or emission in the region of interest. Solution phase experiments are preferred, though it is possible to measure the spectra in other forms such as thin films, powders, etc.

The absortion and emission spectra of InP nanoparticles of 32 Å mean diameter are shown in Fig. 7.5. The absorption spectrum shows a characteristic peak at 590 nm, due to the excitonic absorption (formation of electron–hole pair). The bulk material has an onset of absorption at 918 nm (1.35 eV). The exciton radius of InP is about 10 nm and the particles presented here show strong confinement, which means that the absorption spectrum shifts considerably as a function of size. The spectrum shows a characteristic higher energy transition, above the first excitonic absorption. This indicates the presence of smaller particles, which show lower wavelength absorption. The extent of shift in the absorption spectrum can be used to calculate the particle dimension as shown earlier.

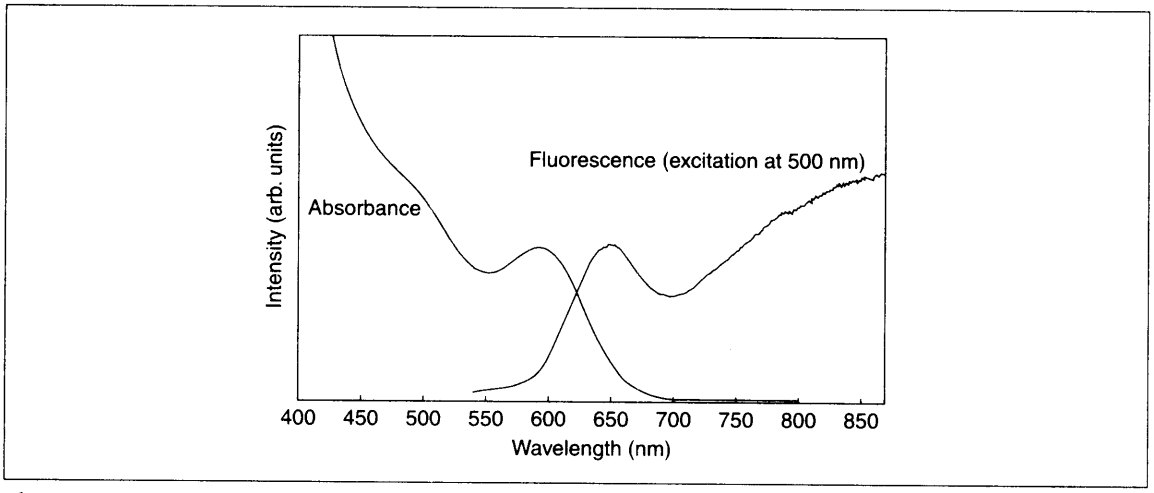

Fig. 7.5: *Absorption and emission spectra of InP nanoparticles. Reused with permission from Micić, et al. (Ref. 4). Copyright 1996, American Institute of Physics.*

The photo-luminescence spectrum of the same sample shows two bands when excited at 500 nm. Two emissions with maxima at 655 nm and above 850 nm are seen. The first one is due to the band gap emission and the other is attributed to radiative surface states produced by phosphorus vacancies.

The optical properties of the quantum dots are heavily affected by the surface of the particles. In the case of such small clusters, the reactivity of the surface atoms will make a thin oxide layer on the surface. This quenches the light emission. In the case of bulk semiconductors, the surface is cleaned by an acid etching. A similar process is undertaken for quantum dots too, by using a mild acid solution (e.g. 5 per cent HF, 10 per cent H_2O in methanol). This creates a nascent surface which shows an intense band edge emission. However, the emission deteriorates over a period of time. The surface can be well protected with ligands which bind strongly such as thiols. In such cases, the material can be stored in air and the solution shows stable emission even after a month.

Both the absorption and emission spectra shift as a function of size. This is a characteristic feature evident in all the nanocrystal samples. Emission has been studied in a range of nanocrystal materials such as ZnO, CdS, CdSe, etc. In the case of CdS, emission occurs in the red region (>600 nm) of the electromagnetic spectrum. The spectrum is attributed to sulphur vacancies. The excitonic emission occurs when more charge carriers are created as in the case of a laser excitation. The emission occurs due to detrapping of electrons. Traps function as charge reservoirs and contribute to an increase in the emission time scale.

Emission is referred to as 'global emission' when the excitation energy is much higher than the absorption maximum of the sample. Note that particles of several diameters are present in the sample and by choosing an energy that is higher than the absorption maximum, a greater percentage of the samples can be excited. Both the photoabsorption and luminescence show enormous size dependence. The linewidths in luminescence can be reduced if the range of particles excited can be reduced. This can be achieved by reducing the size distribution in the sample. In a given size distribution, if the excitation energy is reduced, the range of particles excited reduces and the line width narrows. This technique is called 'fluorescence line narrowing' (FLN).

The PL shows a long lifetime of 28–73 ns at 298 K for 3 nm InP particles. The lifetime increases to 173–590 ns at 13 K. It appears that the emission occurs from a spin-forbidden state. As a result of the larger electron–hole exchange interaction in the excited state, relative to bulk, the excited state (excitonic in nature) splits into a triplet and a singlet. The triplet is lower in energy. However, excitation occurs to the higher lying singlet due to selection rules and relaxation occurs to the triplet from where it emits.

7.4.2 Life Time and Dynamics of the Excited States

The excited states have to decay eventually. The excited state dynamics (subject dealing with stability and rate of decay of the excited states) have been investigated in detail. Radiative and non-radiative processes occur. There can be several ways in which the excited energy can decay and non-radiative processes dominate in the case of nanocrystals whose surfaces are not passivated. Surface defects reduce the quantum efficiency of radiative decay. The defects occur in the form of unsatisfied valencies which provide an easy sink for the charge carriers. In the case of well-passivated nanocrystals, the quantum efficiency can be close to unity, which means that they are almost like dyes. The excited states can lead to charge separation and the charge could reside with an adsorbate species. This is the most critical aspect which decides the photocatalysis of semiconductor nanoparticles.

7.4.3 X-ray Diffraction

X-ray diffraction is the principal method used to identify the phases present in a solid state material. In the case of a nanomaterial, one is making not a new phase, but smaller dimension crystallites of an already known phase. As the dimension of the crystal reduces, the diffraction peaks broaden and in a very small crystallite, there may not be enough planes to diffract. The problem is discussed in Chapter 2. This is shown in the case of InP particles in Fig. 7.6. The extent of broadening can be used to find the diameter of the particles. Therefore, X-ray diffraction as a function of particle dimension is generally carried out. The size of the particles can be found by using the Scherer formula. This may be compared with the data from other techniques such as transmission electron microscopy, scanning electron microscopy, scanning probe microscopy, neutron scattering, dynamic light scattering, etc. The temperature and pressure dependence of powder diffraction is also investigated, which is used to identify phase transitions.

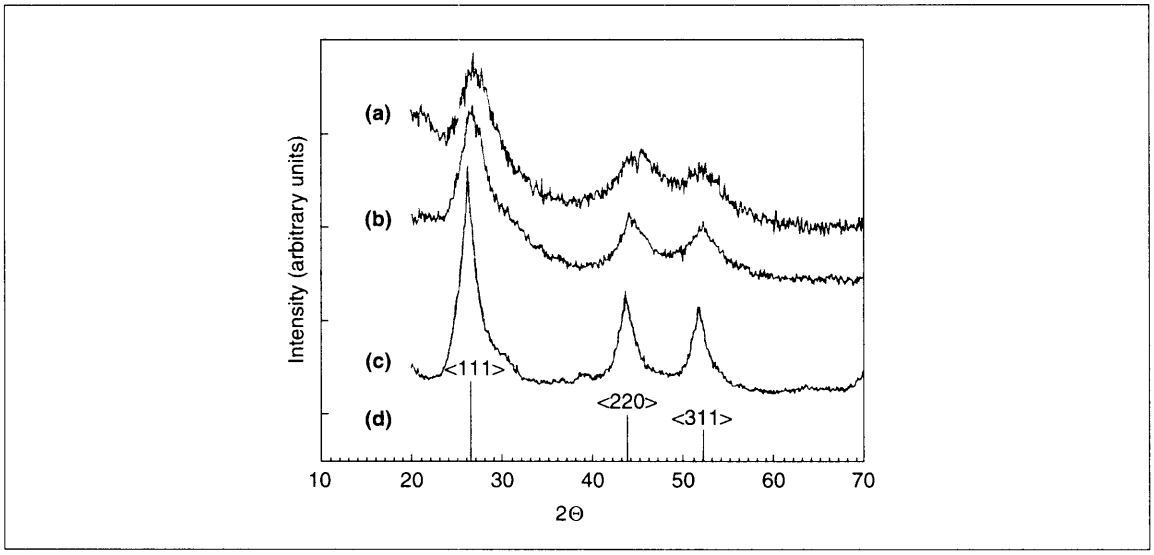

Fig. 7.6: *X-ray diffraction patterns of colloidal InP quantum dots as a function of particle size, (a) 2.5 nm, (b) 3.5 nm and (c) 4.5 nm. The data are compared with the data of bulk InP of zincblende structure (d). While the peak positions and intensities are the same as that of the bulk, the peaks broaden with a decrease in particle size. Reprinted with permission from Micić, et al. (Ref. 5). Copyright (1995) American Chemical Society.*

7.4.4 Transmission Electron Microscopy (TEM)

TEM is the most important characterization tool for a nanomaterial, as nothing can be more convincing than seeing the object. In addition to observing the shape of the object, TEM can reveal the microscopic

structure and atomic composition by using energy dispersive X-ray analysis. In addition, electron energy loss spectroscopy and energy-filtered imaging can provide additional information on the atomic constitution of the materials. These analyses can be done from an area of the order of 1 nm in diameter.

In TEM, it is important to study a large cross section of the sample, not merely one particle. This large area image, as shown in Fig. 7.7, gives the particle size distribution. Generally, a histogram of particle size distribution is plotted, which is more representative of the material synthesized. At higher magnifications, the lattice structure of individual nanoparticles is resolved.

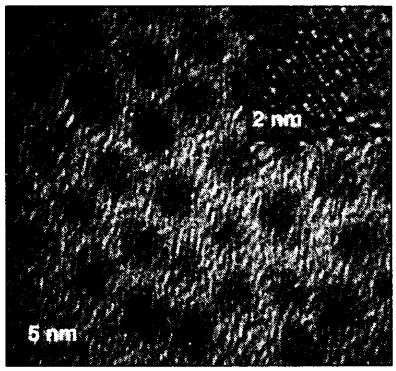

Fig. 7.7: *A collection of CdSe nanoparticles synthesized by chemical route. A magnified image of a single particle is shown as the inset. This gives a lattice-resolved image of the particle. Individual lattice points are observable. Data from the author's laboratory.*

7.4.5 Ancillary Techniques

Several other techniques are routinely used for the characterization of such materials. They include thermogravimetry, differential scanning calorimetry, X-ray photoelectron spectroscopy, Raman spectroscopy, infrared spectroscopy, etc. Thermogravimetry measures the thermal loss/gain of the material when it is subjected to heating at a constant rate. This gives the kinetics of thermal events such as decomposition, reaction, etc. This is also useful in estimating the extent of surface coverage in nanomaterials as the cover is lost in most cases before other thermal processes. Differential scanning calorimetry can be used for evaluating phase changes in the material. Due to the nano dimension, the phase changes occur at a lower temperature, which has been attributed to an increase in the surface energy of the system, which makes the phase unstable. Therefore, phase transitions such as melting occur early. X-ray photoelectron spectroscopy is useful since it provides direct information on the electronic structure. In most of the cases, it is useful in understanding the valence state of the elements present in the sample. Raman and infrared spectroscpies are useful in finding the vibrations in the sample, which are characteristic of the molecular and crystal structures. Thus a combination of techniques is used to characterize the system completely. There are

several other more refined techniques such as small angle X-ray scattering (SAXS), small angle neutron scattering (SANS), and dynamic light scattering (DLS), which are useful in understanding the particle size distribution as well as shape in solutions. X-ray extended absorption fine structure (EXAFS) is used to study the co-ordination and local structure of materials, especially when they are amorphous in nature and where X-ray diffraction is not useful.

7.5 Correlation of Properties with Size

The absorption band edge shifts to the blue as a result of a decrease in the size of the particle. This effect shown in CdS particles is depicted in Fig. 7.8. The effective band gap increases, which explains this shift. The bulk bad gap is 2.42 eV (512 nm) and for all the particles, the measured band gap is higher than this. For several other materials, the band gap has been determined. In all the cases, systematic shifts have been observed. Models have been developed to correlate this shift with the diameter of the particles.

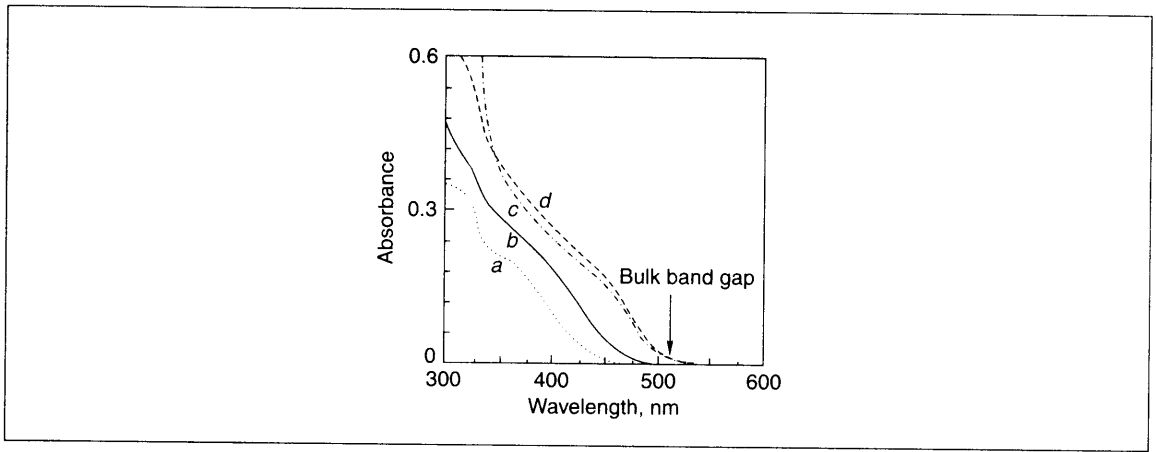

Fig. 7.8: *Shift in the absorption spectra of CdS measured in solution, as a function of the particle dimension. The curves, a, b, c and d correspond to particle dimensions, <25, 30, 37 and >42 Å, respectively. Reprinted with permission from Kamat, et al. (Ref. 6). Copyright (1987) American Chemical Society.*

The simplest of these approaches is to consider the particle in a box model. For one electron confined in a three-dimensional box, the energy levels will be:

$$E_n = h^2/8m_eL^2(n_x^2 + n_y^2 + n_z^2)$$

where

$L = Lx = Ly = Lz$, the length of the box in three dimensions,

n_x, n_y, n_z = the quantum numbers,

m_e= electron mass.

For a spherical semiconductor quantum dot, the energy expression can be derived by using the confined Wannier exciton Hamiltonian and we get:

$$E_n = E_g + n^2h^2/8m^\star R^2 - e^2/4\pi\varepsilon_o\varepsilon R$$

where;

E_g = band gap of the bulk semiconductor,

n = quantum number (1, 2, 3 ...),

h = Planck's constant,

$m^\star = (m_e \times m_h)/(m_e + m_h)$,

m_e = effective mass of electron, m_h = effective mass of hole,

R = radius of the quantum dots,

ε = dielectric constant of the semiconductor.

For the electronic transition from the valence band to the conduction band (n = 1), we can write (note that we have only one electron in the system):

$$E_g(R) = E_g + h^2/8R^2\,(1/m_e + 1/m_h)$$

This neglects the third term.

The increase in the band gap can be given as:

$$\Delta E_g(R) = E_g(R) - E_g = h^2/8R^2(1/m_e + 1/m_h)$$

As shown here, there will be a $1/R^2$ dependence of the shift in the band gap.

Just like the absorption spectral shift, corresponding shifts are observed in emission too. In the case of CdS, the red emission seen is a result of the sulphur vacancies. The peak shifts to blue as a result of a decrease in the particle size. The peak intensity increases and a blue shift occurs as the temperature is decreased. The emission occurs as the electrons are de-excited from the traps. This results in delayed emission.

7.6 Uses

Semiconductor nanocrystals find applications in a number of areas. A summary of the various applications is presented in Fig. 7.9. As can be seen, there are applications in almost every area. Light can be absorbed by using nanoparticles, especially those with band gaps in the visible region. The absorbed light makes an electronic excitation possible in the material, leaving the electron free in the conduction band. This free electron can move throughout the material and can be collected at an electrode. The electron may be put back into the material by a separate event, which creates a category of solar cells. By using efficient dye molecules which have LUMO levels placed near the conduction band of the semiconductor, it is possible to inject the charge from the excited dye molecule into the semiconductor. This has been an active area for some time and the device is referred to as 'dye sensitized solar cell' (Ref. 7).

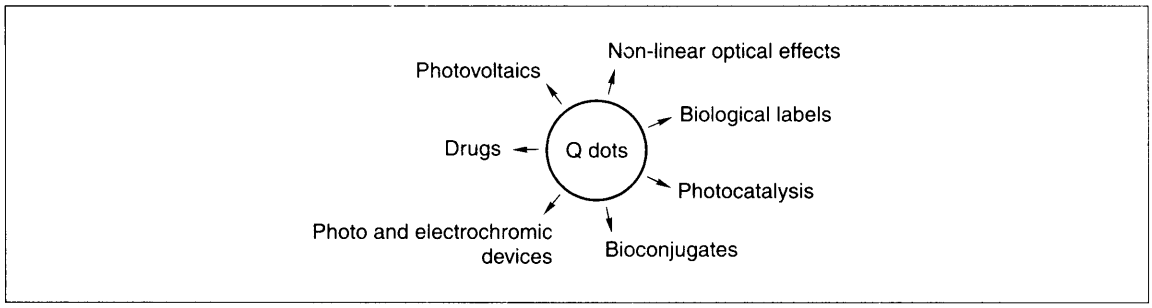

Fig. 7.9: *Diverse applications of quantum dots.*

7.6.1 Chemical Properties

Electron injection into the conduction band can lead to numerous possibilities. The surface of the particles will be covered with functional groups such as hydroxyls in the case of oxides. The hydroxyl groups take up the holes and form hydroxyl radicals, which can result in radical mediated oxidation. Pollutants in water and soil can be efficiently degraded in this way. Photocatalysis can also lead to reduction, using the electron in the conduction band which generates hydroxyl ions or oxide species. All these can make both oxidative and reductive processes feasible. Organic synthesis has utilized the power of semiconductor particles. To quote an example, aromatic ketones and olefins have been converted into alcohols and corresponding saturated compounds. The available electron can be used to fix gas phase CO_2 into organic compounds. In an attempt, CdS nanocrystals have been used to fix CO_2 into benzophenone, acetophenone and benzyl halides producing various compounds (Ref. 8). Various other means of photocatalysis such as the reduction of nitrogen to ammonia, nitrogen oxides to nitrogen, decomposition of pollutants, etc. have also been attempted. In almost all these cases, TiO_2 is used as the photocatalyst. The applications in this field are expanding enormously.

7.6.2 Single Electron Devices

Quantum dots can be used in single electron devices. In order to understand the elementary details of such a system, we consider the example of an electroneutral dot, so-called because the number of electrons that it has is the same as the number of holes. In order to put an electron inside, one has to apply a weak force. Tunneling is the most common means of putting a charge into a device of this kind as the device most often has an insulating barrier around it. The charge that the dot now possesses, $Q = -e$, produces an electric field, ε which repels any incoming negative charge. The fundamental charge is only 1.6×10^{-19} C, but the field it produces on the surface of a dot can be large, of the order of 140 kV on a 10 nm diameter particle. A more important parameter in discussing single electron phenomenon has been recognized as the charging energy, $E_c = e^2/C$. At smaller dimensions, the electronic energy states in the

material are quantized. The energy required for the addition (of charge) is a sum of the charging energy and the electron kinetic energy in the material. In the larger size regime, of the order of 100 nm, the addition energy is dominated by the charging energy and the energy required for addition is of the order of μeV. Thus thermal energy is enough to do the job. Therefore, single electron effects will be manifested only at lower temperatures when thermal energy is small. However, in the lower size regime of the order of 10 nm, addition energy will be of the order of meV and will be dominated by electron kinetic energy or will become comparable to the charging energy.

Single electron transition and corresponding effects are manifested dramatically in current-voltage measurements of nanocrystals. Imagine that a device structure is constructed in such a way that a single nanoparticle is trapped between an electron source and an electrode. As the electrode is separated at a large distance such that appreciable tunneling does not occur, a potential U is applied. If one measures the charge of the particle, Q as a function of the 'external charge', $Q_e = CU$, we get a step-like function. This is called the 'Coulomb staircase'. Q is a step function of U, with the distance between the neighboring steps = e. $\Delta Q = e$ or $\Delta U = e/C$. However, when thermal energy becomes comparable to the charging energy, the thermal fluctuations smear out the staircase.

Such a staircase implies that electrons can be transferred one at a time. However, the device by itself cannot be used for properties such as rectification or memory. These properties can be attained only by the use of more complicated devices such as single electron transistors, single electron traps, etc. The fundamental aspect of such device structures is the capability to charge or discharge nanosized regions selectively.

Review Questions

1. Can a quantum dot be made with a metallic element?
2. How is quantum confinement manifested in various measurements?
3. How would one make and stabilize a quantum dot?
4. What are the different types of quantum dots investigated?
5. What makes quantum dot luminescence attractive?
6. How do we correlate absorption spectra with size of the quantum dot?
7. What are the unique chemical properties of quantum dots? Give specific examples and illustrate how these are possible.
8. Why functionalize these particles?
9. How do make biocompatible quantum dots?

References

1. Sastry, M., A. Ahmad, M.I. Khan, *et al.*, *Current Science*, **85** (2003), p. 162.
2. Herron, N., J.C. Kalabrase, W.E. Farneth and Y. Wang, *Science*, **259** (1993), p. 1426.
3. Liu, D. and P.V. Kamat, *J. Electroanal. Chem. Interfacial Electrochem.*, **347** (1993), p. 451.
4. Mićić, O.I., J.R. Sprague, Z. Lu and A.J. Nozik, *Appl. Phys. Lett.*, **68** (1996), p. 3150.
5. Mićić, O.I., J.R. Sprague, C.J. Curtis, K.M. Jones, J.L. Machol and A.J. Nozik, *J. Phys. Chem.*, **99** (1995), p. 7754.
6. Kamat, P.V., N.M. Dimitrijevic and R.W. Fessenden, *J. Phys. Chem.*, **91** (1987), p. 396.
7. O'Regan, B. and M. Gratzel, *Nature*, **353** (1991), pp. 737–739.
8. Kanemoto, M., H. Ankyu, Y. Wada and S. Yanagida, *Chem. Lett.*, **2113** (1992); H. Fugiwara, H. Hosokawa, K. Murakoshi, Y. Wada, S. Yanagida, T. Okada and H. Kobayashi, *J. Phys. Chem. B.* **101** (1997), p. 8270.

Additional Reading

1. Brus, L., *J. Phys. Chem.*, **90** (1986), p. 2555.
2. Henglein, A., *Chem. Rev.*, **89** (1989), p. 1861.
3. Alivisatos, A.P., *J. Phys. Chem.*, **100** (1996), p. 13226.
4. Nirmal, M. and L. Brus, *Acc. Chem. Res.*, **32** (1999), p. 407.
5. Klabunde, Kenneth J., (ed.) (2001), *Nanoscale Materials in Chemistry*, Wiley, New York.
6. Nalwa, Hari Singh (ed.) (2001), *Nanostructured Materials and Nanotechnology*, (ed.) (2002), Academic Press, New York. See articles of P.V. Kamat, K. Murakoshi, Y. Wada and S. Yanagida; O.I. Mićić and A.J. Nozik as well as V.L. Klimov in the book dealing with the subject.
7. Several articles in Nalwa, Hari Singh (ed.) (2004), *Encyclopedia of Nanoscience and Nanotechnology*, Academic Press, New York.
8. Liz-Marzan, Luis M. and P.V. Kamat, (2003), *Nanoscale Materials*, Kluwer Academic Publishers, Boston.
9. Rao, C.N.R., A. Muller and A.K. Cheetham (eds) (2004), *The Chemistry of Nanomaterials: Synthesis, Properties and Applications*, Wiley–VCH, Weinheim.

Chapter 8

Monolayer-Protected Metal Nanoparticles

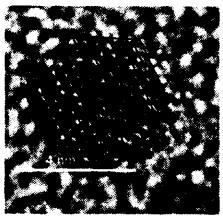

The synthesis of redispersible nanomaterials has expanded the scope of colloidal chemistry. They can be treated just as molecules, which may be stored as powders, dispersed in solvents, reacted with suitable molecules, etc. In effect, they act as reagents. Such materials can be characterized by spectroscopic and microscopic techniques. Any property can be incorporated in such materials by functionalizing them with suitable protecting molecules. This creates a lot of possibilities for the applications of such systems. The assembly of such systems into ordered structures is interesting. Such ordered arrays are expected to show unusual properties that are entirely different from those of individual nanocrystals.

Learning Objectives

- What are the differences between clusters with and without monolayers?
- How does functionality make a difference?
- What are the applications of clusters?
- What are metal cluster superlattices?

8.1 Introduction

In 1857 Faraday made colloidal gold by reducing the aqueous solution of $AuCl_4^-$ with phosphorus in CS_2 (Ref. 1). Since then several methods have become available for the synthesis of colloidal gold particles. The most popular one is the citrate reduction method of Turkevitch (Ref. 2). Here a solution of the gold or silver salt (typically 1 mM) is boiled with a higher concentration (typically 1 M) of sodium citrate for a few minutes. This results in the formation of metal colloids of 10–50 nm diameter, and the size can be varied by altering synthetic parameters. This colloidal solution is stable for several months (the gold colloid is much more stable than that of silver). Here the stability is due to an electrical double layer surrounding the metal surface. This layer is dynamic and the colloid is stable as long as the conditions are not altered greatly. For example, if we precipitate the colloid, the material cannot be re-dispersed. Precipitation leads to aggregation as the stabilizing ionic layer is easily disturbed. A stable colloidal particle which can be precipitated, dried and re-dispersed, or in effect one that has similar characteristics as a molecule, generated interest for a long time. The 3D monolayers or monolayer-protected metal clusters

(MPCs) belong to this category of materials. They are molecular materials, wherein the constituting monolayer-protected clusters or nanoparticles behave like molecules. 3D is to distinguish these from the corresponding 2D monolayers, which are grown on planar surfaces.

8.2 Method of Preparation

By combining this two-phase method of Faraday and the technique of phase transfer catalysis, Brust, *et al.*, prepared dodecanethiol-protected gold nanoparticles with a core size in the range 1–3 nm (Ref. 3). $AuCl_4^-$ was transferred to toluene using tetra octyl ammonium bromide as the phase transfer agent. The phase-transferred Au^{3+} is then reduced in the presence of the surfactant, octadecanethiol using $NaBH_4$ as the reducing agent (see Fig. 8.1).

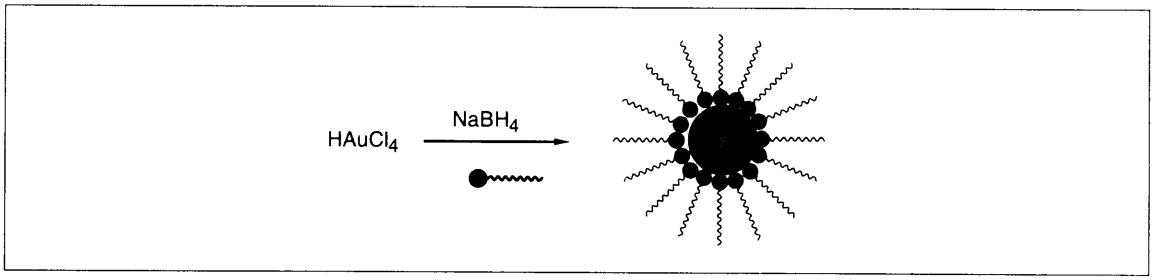

Fig. 8.1: *Schematic showing the Brust method of preparing monolayer-protected clusters.*

The overall reaction is:

$$AuCl_4^-(aq) + N(C_8H_{17})_4^+ \text{ (toluene)} \rightarrow N(C_8H_{17})_4^+AuCl_4^- \text{ (toluene)}$$

$$mAuCl_4^- \text{ (toluene)} + nC_{12}H_{25}SH\text{(toluene)} + 3me^- \rightarrow (Au_m)(C_{12}H_{25}S)_n\text{(toluene)} + 4mCl^{-1}(aq)$$

The material formed is a dark brown powder with a waxy texture. This may be referred to as Au@DDT, the @ symbolism means that DDT covers Au (DDT is dodecane thiol, $C_{12}H_{25}SH$). The material is redispersible in common organic solvents and can be purified by gel filtration chromatography with sepharose 6B/toluene. The size of the gold core can be controlled by varying the metal ion to ligand ratio. A large thiol/gold ratio leads to the formation of smaller nanoparticles. Various ligands other than thiols have been used to prepare 3D SAMs.

8.3 Characterization

Various tools have been used to characterize SAMs. These include UV/vis spectroscopy, transmission electron microscopy, X-ray diffraction, mass spectrometry, infra-red spectroscopy, X-ray photoelectron spectroscopy, nuclear magnetic resonance spectroscopy and differential scanning calorimetry.

UV-vis absorption spectroscopy has been used to characterize the core of the material. Noble metal nanoparticles show surface plasmon resonance due to the coherent oscillation of the conduction band electrons excited by electromagnetic radiation (Fig. 8.2). This happens when the core size is comparable to the mean free path of the electron. The frequency of the plasmon absorption band (ω_p) is related to the free electron density by the equation $\omega_p^2 = \pi Ne^2/m$, where N is the free electron density, e is the electron charge and m is its effective mass. Mie explained this phenomenon by solving Maxwell's equations for the absorption and scattering of the electromagnetic radiation by spherical particles (Ref. 4). More details on this can be found in the chapter on Core Shell Nanoparticles (Chapter 9).

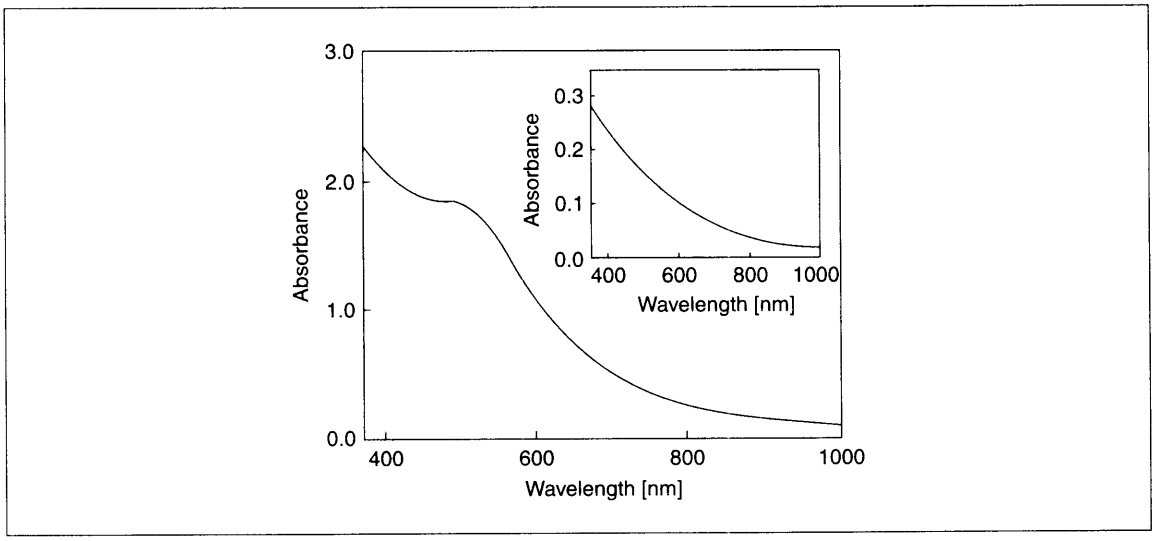

Fig. 8.2: *UV-vis spectrum of Au@hexanethiol showing the presence of surface plasmon resonance at 520 nm. Inset shows the spectrum for sub-nanosized metal clusters for which the plasmon is very weak. From the author's work.*

The plasmon absorption band is characteristic of the size and shape of nanoclusters. Anisotropic particles such as metal nanorods show the presence of two plasmon features, namely 'transverse', due to the coherent oscillation along the short axis, and 'longitudinal' due to the oscillation along the long axis. The intensity of the longitudinal plasmon band is large and its position varies with the length of the rod.

Techniques like TEM, XRD, AFM, STM, etc. have been used to derive information on the structure of the metal core. High resolution transmission electron microscopy at lattice resolution on size-selected gold nanocrystallites showed FCC packing of atoms in the gold core with a mixture of particle shapes with predominantly truncated octahedral, cuboctahedral and icosahedral structures. The octahedral core will have eight (111) planes and the six corners will be truncated by (100) planes. The high radius of curvature of the core suggests that the monolayer chain density decreases as we move away from the metal core. Thus the terminal methyl groups have enough orientational freedom. This is again supported by the fact that the hydrodynamic radius of the metal nanoparticles is lower than that calculated by assuming the

monolayer to be a straight chain. TEM gives the mean diameter (d) of the particles which can be used to calculate the mean number of atoms (N) in the core using the relationship, $N_{Au} = 4\pi(d/2)^3/V_{Au}$.

X-Ray photoelectron spectroscopy has been used to find out the oxidation state of gold in the material. The Au $4f_{5/2}$ (87.5 eV) and Au $4f_{7/2}$ (83.8 eV) values are characteristic of Au^0 in the material. This shows that largely gold is present in the Au^0 state in the core. The absence of the Au(I) band at 84.9 eV (for Au $4f_{7/2}$) ruled out the possibility of gold sulphide character of the Au-S bond.

IR spectroscopy is a powerful tool used to study the structure of the adsorbate on the metal surface. An increase in the intensity of the methylene stretching vibrations with an increase in the chain length indicates that the structural integrity of the alkanethiol was maintained during the cluster formation. The position of the d_+ and d_- methylene bands indicates if the alkane chain is crystalline or not. Thiols with carbon atoms of less than eight show a liquid-like structure. In the case of longer thiols, the values 2850 cm^{-1} and 2920 cm^{-1} (for d_+ and d_-) are close to the values of crystalline alkanes. The high crystallinity indicates the all-trans arrangement of the methylene chains. The merging of the r_+ and r_- bands indicates that the terminal methyl group has enough rotational freedom. The disappearance of S-H stretching frequency at 2650 cm^{-1} indicates that the thiols attach to the metal surface as thiolates.

^{13}C NMR spectra of alkane thiol stabilized clusters for three different alkyl chain lengths showed that the peak narrows down as the distance of the carbon from the gold surface increases. For example, among C_6, C_{12} and C_{16} capped clusters, the line width of the methyl resonance at 14 ppm was minimum for hexadecane thiol capped gold. ^{13}C NMR spectrum of octane thiol capped gold nanoparticles showed peaks only for carbon beyond C_γ. The resonances corresponding to the carbons close to the gold surfaces, namely C_α, C_β and C_γ, did not show up in the spectra. This is because they were flattened into the base line. The factors which can affect the distance dependent broadening are dependence of spin lattice relaxation rate on magnetic field anisotropy, chemical shift anisotropy and residual heteronuclear dipolar interactions. Among these factors, the major contribution was from residual heteronuclear dipolar interactions.

MPCs display current due to double layer charging of the metal core. This is due to the extremely small sub-atto Farad capacitance of MPCs. The double layer charging occurs as a series of one electron, approximately evenly spaced, current peaks as shown in Fig. 8.3. This results from the single electron changes in the charge state of the core. For the differential pulse voltammetry of a dilute solution of MPCs, peaks will be observed for the addition or subtraction of each electron. The space between the successive peaks in the differential pulse voltammetry is e/C_{dlu}, where e is the electron charge and C_{dlu} is the double layer capacitance.

One can charge the core of the MPCs electrochemically in a solvent in the presence of a supporting electrolyte. The solvent is then removed and the supporting electrolyte is washed away. Such positively or negatively charged MPCs can act as oxidizing as well as reducing agents. These charged MPCs are reasonably stable and can be handled like usual compounds. Murray, *et al.*, (Ref. 6) studied ligand exchange reactions on electrochemically charged MPCs. They found that the rate as well as the extent of exchange increased with an increase in the positive charge on the core. Mixing MPCs with different core charges results in the transfer of electrons between the MPCs resulting in a solution with a potential determined by the stoichiometry of the mixture and Nernst equation.

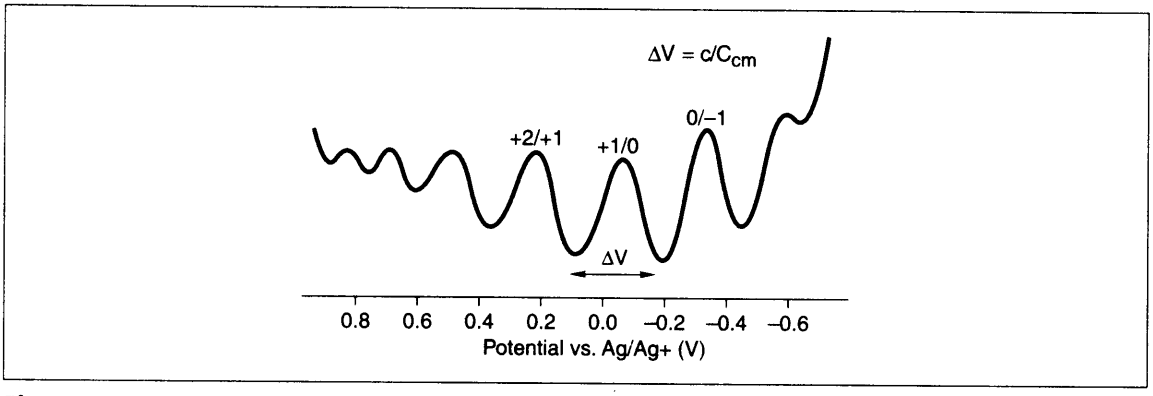

Fig. 8.3: *Differential pulse voltammetry of 0.1 mM C_6MPCs in CH_2Cl_2 measured at a 1.6 mm diameter Pt working electrode using 50 mM Bu_4NClO_4 as the supporting electrolyte. Reprinted with permission from Song, et al. (Ref. 5). Copyright (2002) American Chemical Society.*

The DSC of the alkanethiol-capped gold nanoparticles with alkane thiols with chain lengths varying from C_{12} to C_{20} are shown in Fig. 8.4. The broad endotherm is caused by the order–disorder transition associated with the hydrocarbon chain. The transition temperature as well as the transition enthalpy

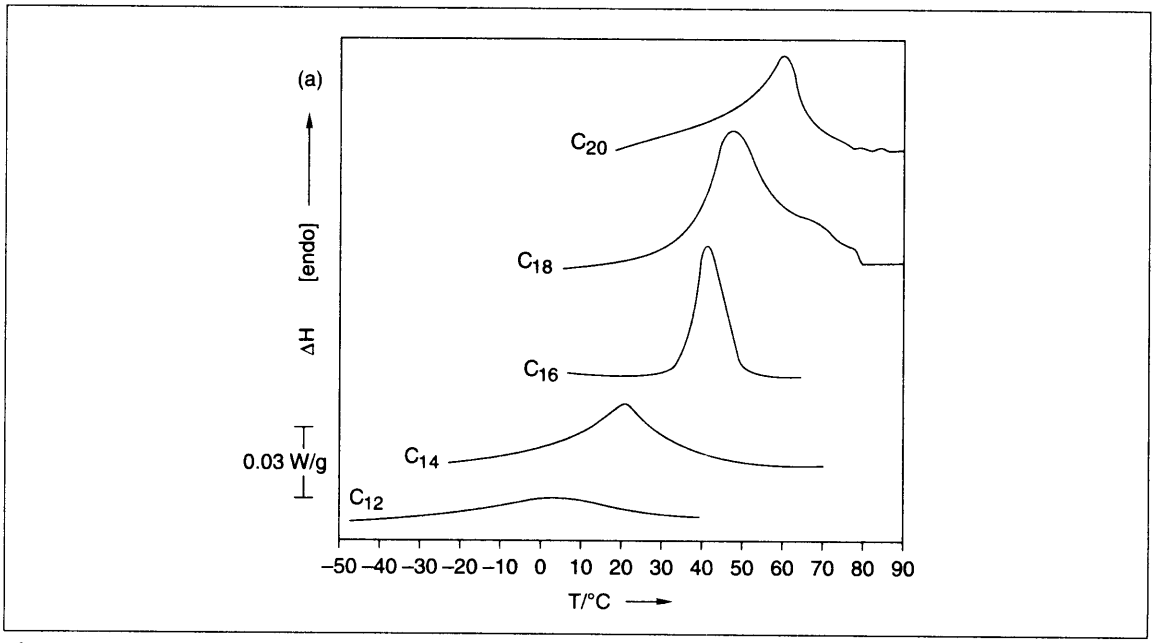

Fig. 8.4: *Differential scanning calorimetry of alkanethiol capped gold clusters showing the peak corresponding to the alkyl chain melting. The melting temperature as well as the transition enthalpy increase with an increase in the chain length of the thiol. Reprinted with permission from Templeton, et al. (Ref. 6). Copyright (2000) American Chemical Society.*

increase with the chain length. Alkyl chains below 12 carbons do not show the melting of the hydrocarbon chain. Apart from this, another melting is observed above 100 °C. This is due to the small fraction of the superlattice (see later) present in the sample.

The enthalpy of the superlattice melting can be very high due to the high cohesive energy of such systems. As one can see from the cartoon structure of the superlattice in Fig. 8.5, the ordered portion of the alkyl chain can be either at the end or in between the two clusters.

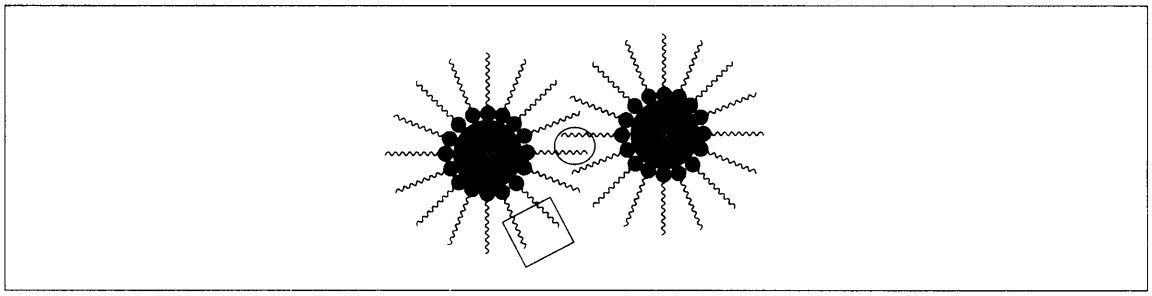

Fig. 8.5: *Cartoon of thiol protected gold clusters showing the possible regions of crystallinity. Circle shows the region of crystallinity because of the interdigitation of alkyl chains and square shows the possibility of interstitial folding.*

8.4 Functionalized Metal Nanoparticles

The synthesis of functionalized nanomaterials has been receiving considerable attention during the past few years. Functionalization can be either through a ligand exchange reaction or using modified thiol as the capping agent in the Brust method. Various photoactive molecules have been attached to the surface of gold using the thiol end group and such structures are shown in Fig. 8.6. These include derivatives of porphyrenes (Ref. 7), fullerenes (Ref. 8), pyrenes (Ref. 9), stilbenes (Ref. 10), fluorenes (Ref. 11) resorcinarenes (Ref. 12), azobenzenes (Ref. 13), etc.

Photoswitchable gold nanoparticles with a double shell structure in which the inner shell is made of spiropyran, have been used to control the binding and release of the outer shell of amino acids. Under dark conditions, a majority of the spiropyran exist in the close ring form. This non-polar form does not have color. When irradiated with light, spiropyran (SP) changes to the highly polar-colored merocyanin (MC) form. This open ring merocyanin can form a complex with amino acids which helps in forming a further layer of amino acid around the gold nanoparticles (Fig. 8.7). Such systems can be possible candidates for light-mediated binding and release of amino acid derivatives.

Another interesting property was observed in pyrene methyl amine-capped gold nanoparticles. The fluorescence of pyrene was found to increase when attached to the metal surface. This was entirely different from the normal trend wherein heavy metals quench the fluorescence. The binding of nitrogen onto the

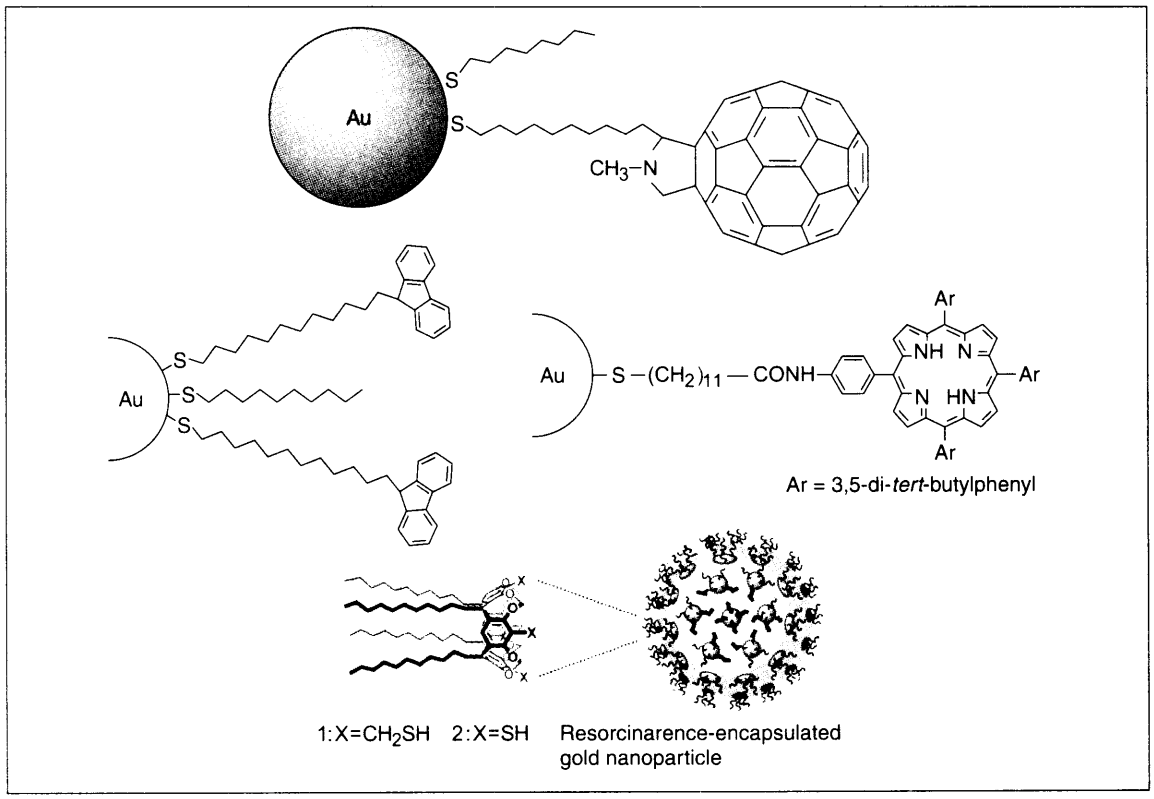

Fig. 8.6: *Various functionalized nanoparticles, with their chemical functionalities.*

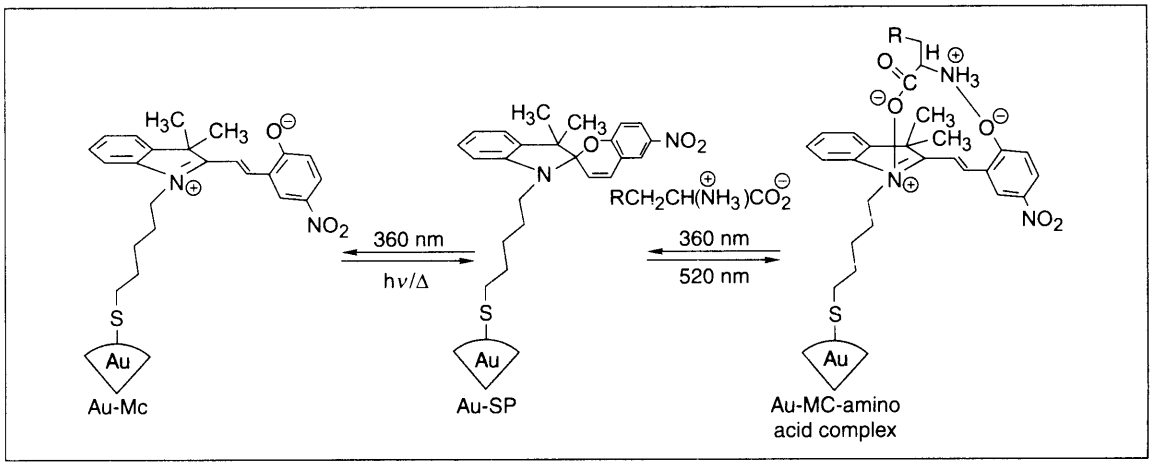

Fig. 8.7: *Reversible binding of amino acids with spiropyran capped gold nanoparticles. Reprinted with permission from Ipe, et al. (Ref. 14). Copyright (2003) American Chemical Society.*

gold suppresses the electron transfer between the nitrogen and the pyrene ring as shown by the arrows in Fig. 8.8. This results in enhanced fluorescence.

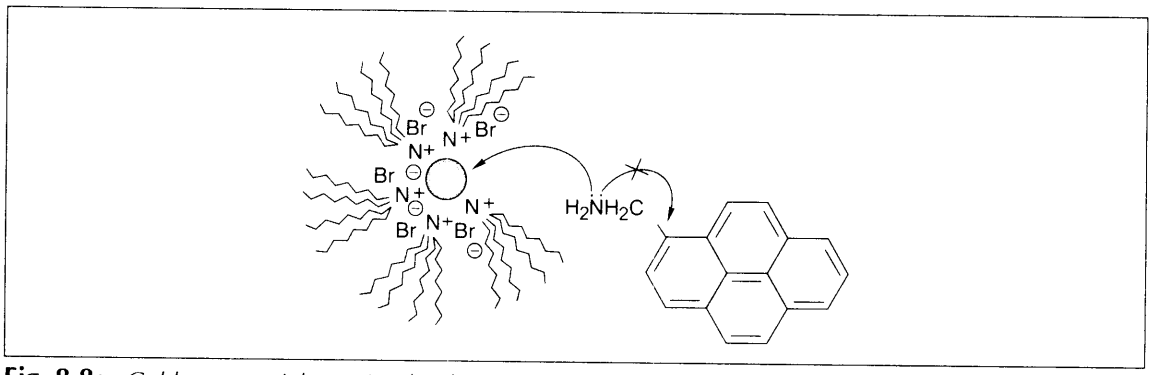

Fig. 8.8: *Gold nanoparticles-assisted enhancement of fluorescence in pyrene methyl amine. Due to the attachment of nitrogen onto the nanoparticles, conjugation between lone pair on nitrogen and the pyrene ring is blocked. This is indicated by an arrow with a cross mark. Reprinted with permission from Thomas and Kamat (Ref. 15). Copyright (2000) American Chemical Society.*

8.5 Applications

Gold nanoparticles have very high extinction coefficients, and the color change during the transition of nanoparticles from the dispersed to the aggregate state is quite evident. Hence the coupling of nanoparticles with ionophores gives better sensors. The sensing of a particular ion by the ionophores will be seen as a color change. Crown ethers in combination with gold nanoparticles have been used as K^+ ion sensor. K^+ has the ability to form 1:2 adducts with crown ethers attached to adjacent nanoparticles as shown in Fig. 8.9. This results in aggregation and the color changes from dark brown to purple (Ref. 16).

Bidentate ligands attached to gold nanoparticles provide it specificity to a particular ion due to its capability to form chelate complexes. The chelation leads to aggregation and color change, which can be used to find the concentration of the ion. The scheme in Fig. 8.10(a) shows the Li^+ ion assisted aggregation of gold nanoparticles. The corresponding TEM picture is shown in Fig. 8.10(c).

Toxic heavy metal ions such as lead, cadmium and mercury can be detected by using gold nanoparticles. In the presence of metal ions, gold nanoparticles aggregate through chelation of the ions with the carboxyl group on adjacent nanoparticles as shown in Fig. 8.11. This ion templated chelation process changes the color of the solution. It also changes the Rayleigh scattering response from the medium. This chelation can be reversed through the addition of a strong metal ion chelator such as EDTA.

Temperature-sensitive polymers have been grafted onto the surface of nanoparticles to make molecular thermometers. A commonly used functional polymer is poly-N-isopropyl acryl amide. This polymer has a lower critical solution temperature (LCST) of 35 °C. Below 35 °C, hydrogen bonding between the water

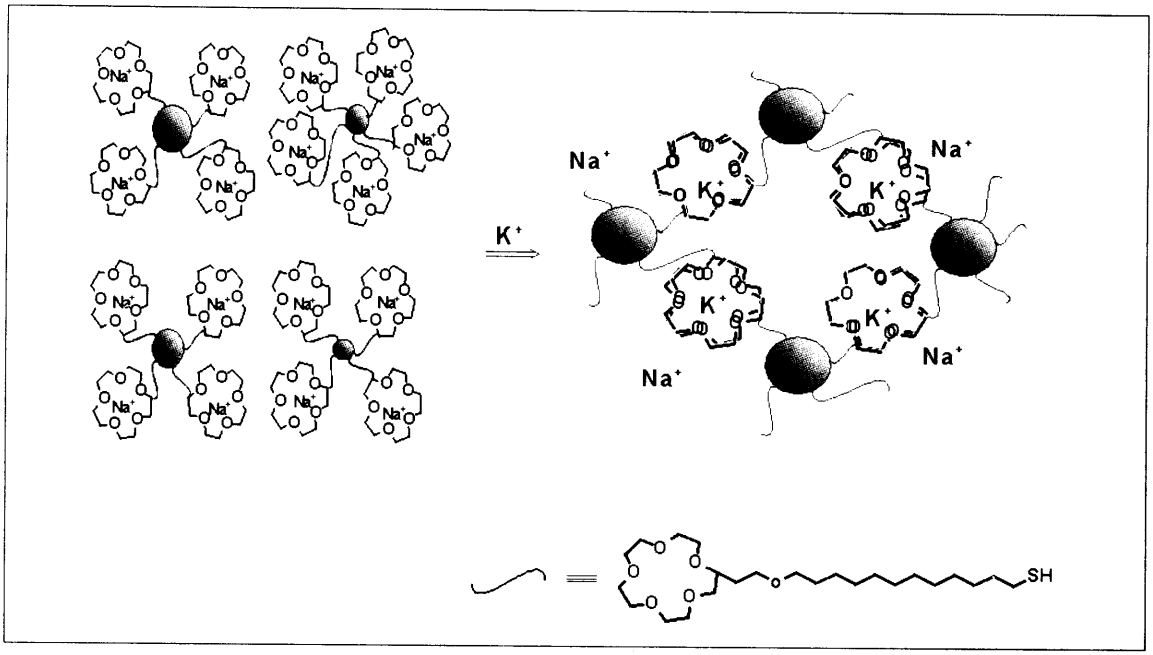

Fig. 8.9: *Schematic showing the sensing of potassium ion by crown ether functionalized gold nanoparticles, The addition of K^+ leads to the formation of adducts which brings about the aggregation of nanoparticles resulting in a color change. Reprinted with permission from Lin, et al. (Ref. 16). Copyright (2002) American Chemical Society.*

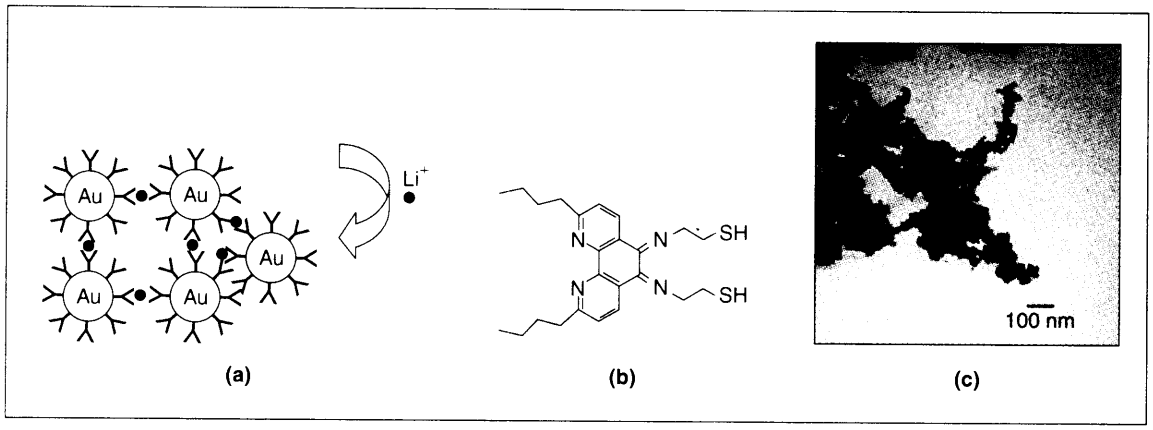

Fig. 8.10: *Selective detection of lithium ion by gold nanoparticles. The structure of the ligand used is shown in Fig. 8.10(b). Fig. 8.10(c) shows the TEM picture of the aggregate. Reprinted with permission from Obare, et al. (Ref. 17). Copyright (2002) American Chemical Society.*

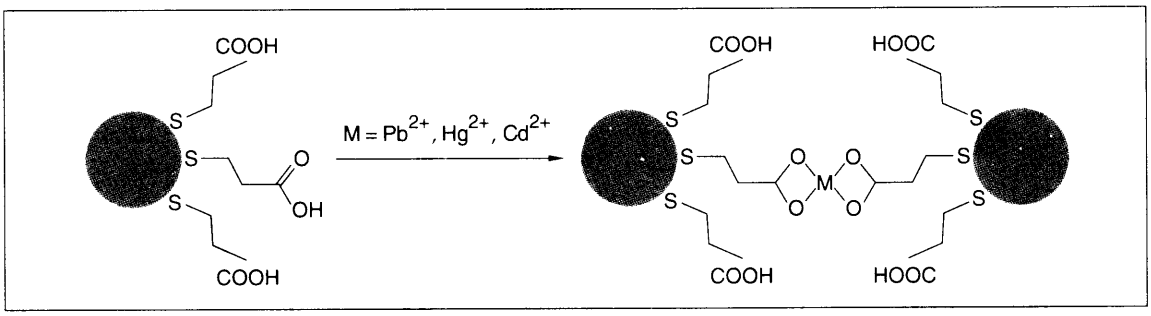

Fig. 8.11: *Ion-assisted chelation for the detection of heavy metals, Picture taken from the Table of Contents entry link of Ref. 18. Copyright (2001) American Chemical Society.*

and the polar groups makes the polymer soluble in water. Above 35 °C the hydrophobic interaction predominates and throws out all the water molecules, thus acting as a molecular thermometer. The coil-to-globule chain transition taking place as a result of the changes in the surrounding temperature is schematically shown in Fig. 8.12.

8.6 Superlattices

Superlattice is a periodic, synthetic multi-layer, wherein a unit cell, consisting of successive layers that are chemically different from their adjacent neighbors, is repeated. These materials are characterized by their double periodicity in the structure, periodicity of atoms in the angstrom level, and periodicity of nanocrystals in the nanometer level.

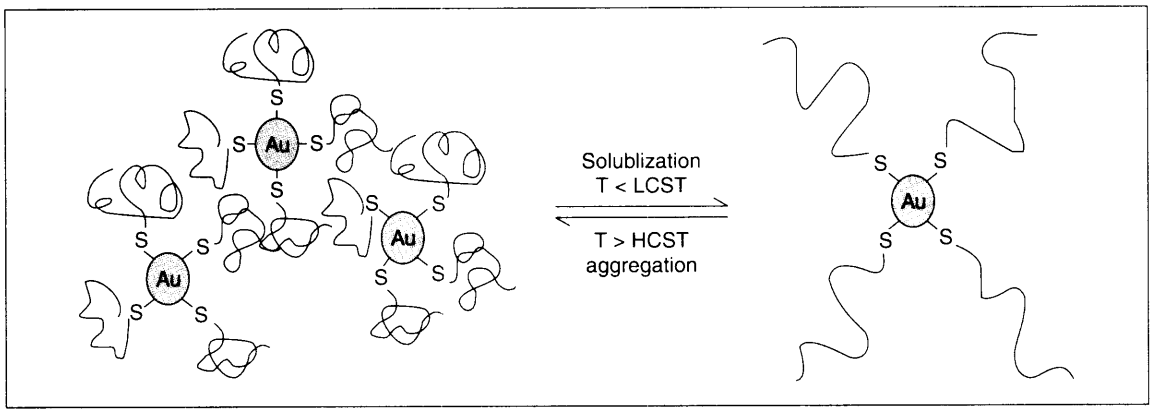

Fig. 8.12: *Temperature sensor based on gel-coated nanoparticles. HCST refers to higher critical solution temperature. Reprinted with permission from Zhu, et al. (Ref. 19). Copyright (2004) American Chemical Society.*

In order to allow the superlattice formation to occur, the van der Waals interaction between the particles should be sufficiently strong to create a secondary minimum M_2 in the potential energy–distance curve as shown in Fig. 8.13. The secondary minimum is very shallow for smaller particles. Hence during the growth of the particles, the system crosses the small energy barrier P and is taken to stable minimum M_1 which results in irreversible aggregation.

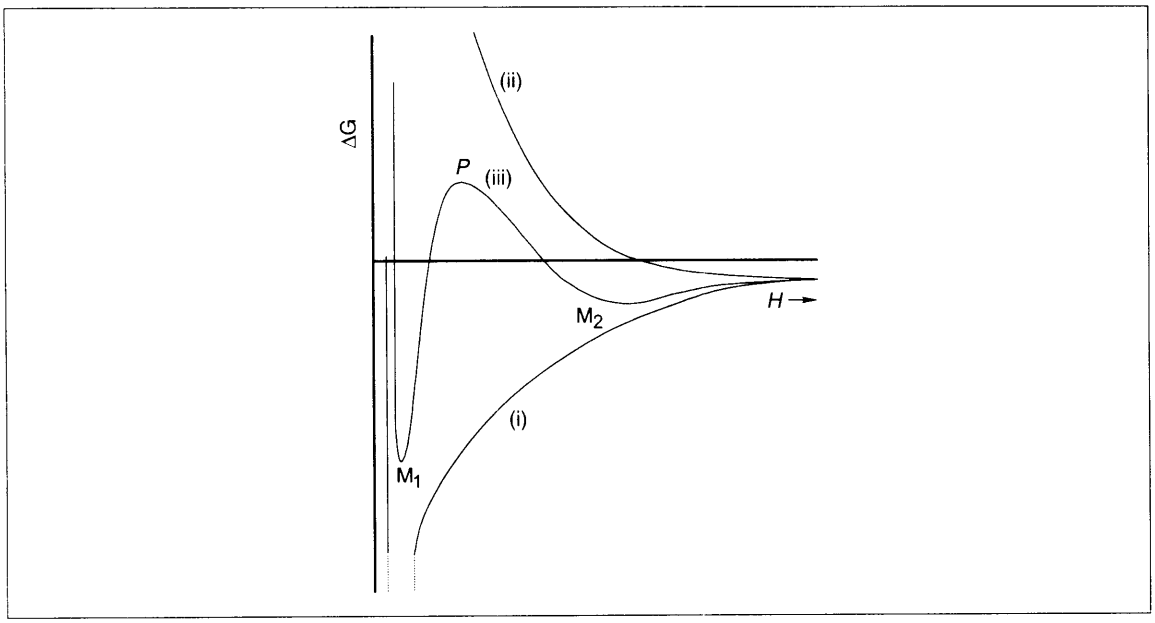

Fig. 8.13: *Potential energy–distance curve showing the resultant interaction energy (iii) due to contribution from attractive (i) as well as repulsive forces (ii). M_2 refers to the shallow minimum which can lead to particles associated reversibly and M_1 refers to the stable minimum leading to irreversible aggregation. H is the interparticle distance and ΔG denotes the change in Gibbs free energy. From Ref. 20.*

Monodispersity is another important factor that controls the formation of superlattice. Even though the Brust method gives redispersible materials, the particle distribution is very large. Hence size selective separation is required to make monodisperse particles. The method developed by Murray, *et al.*, 1993, (Ref. 21), facilitates the synthesis of monodisperse particles. Here the metal–organic precursors are injected into a hot solution containing co-ordinating ligands like trioctyl phosphine. Extensive research has taken place on CdSe superlattices that have been prepared by using this method (Ref. 22). Figure 8.14 (Plate 5) shows the superlattice prepared from CdSe nanoparticles.

When a drop of the solution of monolayer-protected cluster in a volatile organic solvent is placed on a plane surface and allowed to evaporate under controlled conditions, the particle starts coming closer, the individual nanocrystals start nucleating and the crystal starts growing. This is followed by an annealing process which results in the formation of superlattices.

In hydrophobically-modified SAMS. hard sphere repulsion and van der Waals forces assist the formation of superlattices. The self-organization of monolayers leads to an assembly of the chains on the crystal planes of the nanocrystals. Such assemblies of adjacent clusters can interact, forming a well-organized superlattice structure as shown in Fig. 8.15. The structure of such assemblies and the phase behavior of such systems has been the subject of intense investigation in our research group (Ref. 24). The superlattice structure undergoes a first order phase transition and can reverse into a liquid phase. Such a liquid phase exists for a narrow range of temperatures. Beyond a particular temperature, the alkyl chains possess orientational freedom in the superlattice structure.

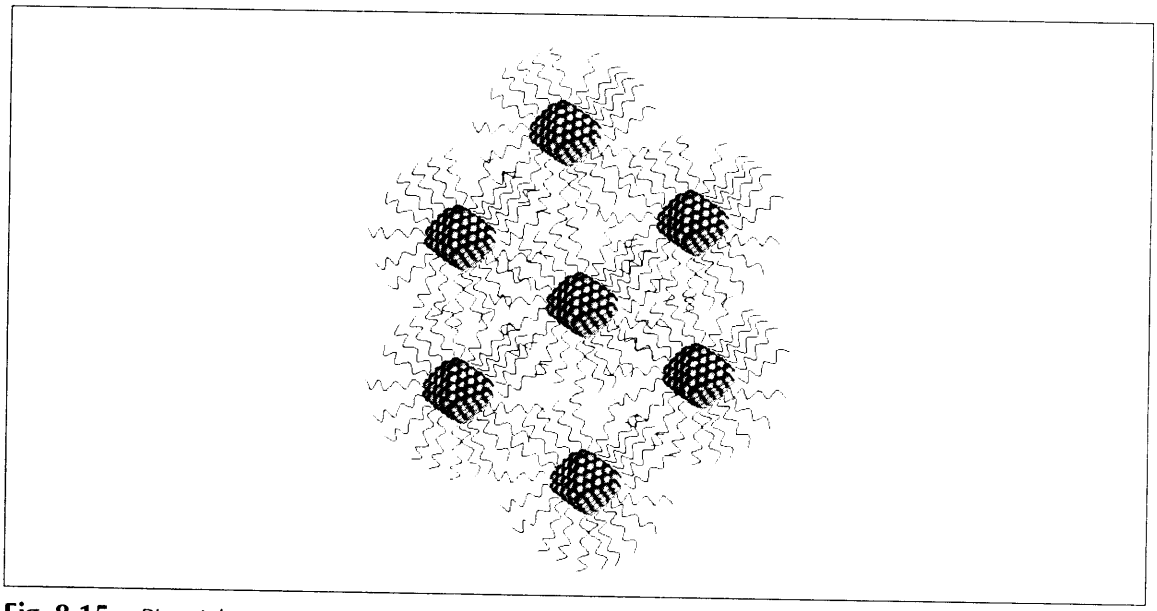

Fig. 8.15: *Pictorial representation of a superlattice.*

The formation of a superlattice is easy if the surface of the nanoparticle is modified with thiols with the terminal group capable of forming hydrogen bonds. Kimura has observed the hydrogen bond-mediated formation of superlattices in mercaptosuccinic acid modified gold nanoparticles (Ref. 26). The superlattice formation in this case is believed to be assisted by the water clusters trapped in the tetrahedral and octahedral cavities that are created by the hexagonal close packing of the constituent nanocrystals. The optical micrograph of the crystals thus obtained is shown in Fig. 8.16.

Digestive ripening is another way of making 'superlattice' (Ref. 27). In this method, the already prepared nanoparticles are refluxed in a solvent with ligands capable of acting as digestive ripening agents. This includes thiols, amines, alcohols, alkanes and silanes. Among the ripening agents, thiols are found to be better than the others. In this process, larger nanocrystals grow at the cost of smaller ones. Thus the growth takes place in size, and not in number. The TEM picture of the particles during each step is shown in Fig. 8.17.

References

1. Faraday, M., *Phil. Trans.*, **147** (1857), p. 145.
2. Turkevitch, J., P.C. Stevenson and J. Hiller, *Discuss Faraday Soc.*, **11** (1951), p. 55.
3. Brust, M., M. Walker, D. Bethell, D.J. Schffrin and R.J. Whyman, *J. Chem. Soc., Chem. Commun.*, **801**, (1994).
4. Mie, G., *Ann. Phys.*, **25** (1908), p. 377.
5. Song, Y. and R.W. Murray, *J. Am. Chem. Soc.*, **124** (2002), p. 7096.
6. Templeton, A.C., W.P. Wuelfing and R.W. Murray, *Acc. Chem. Res.*, **33** (2000), p. 27.
7. Imahori, H., M. Arimura, T. Hanada, Y. Nishimura, I. Yamazaki, Y. Sakata and S. Fukuzumi, *J. Am. Chem. Soc.*, **123** (2001), p. 335.
8. Fujihara, H. and H. Nakai, *Langmuir*, **17** (2001), p. 6393.
9. Wang, T., D. Zhang, W. Xu, J. Yang, R. Han and D. Zhu, *Langmuir*, **18** (2002), p. 1840.
10. Zhang, J., J.K. Whitesell and M.A. Fox, *Chem. Mater.*, **13** (2001), p. 2323.
11. Gu, T., T. Ye, J.D. Simon, J.K. Whitesell and M.A. Fox, *J. Phys. Chem. B*, **107** (2003), p. 1765.
12. Balasubramanian, R., B. Kim, S.L. Tripp, X. Wang, M. Lieberman and A. Wei, *Langmuir*, **18** (2002), p. 3676.
13. Manna, A., P.L. Chen, H. Akiyama, T.X. Wei, K. Tamada and W. Knoll, *Chem. Mater.*, **15** (2003), p. 20.
14. Ipe, B., S. Mahima and K.G. Thomas, *J. Am. Chem. Soc.*, **125** (2003), p. 7174.
15. Thomas, K.G. and P.V. Kamat, *J. Am. Chem. Soc.*, **122** (2000), p. 2655.
16. Lin, S.Y., S.W. Liu, C.M. Lin and C.H. Chen, *Anal. Chem.*, **74** (2002), p. 330.
17. Obare, S., R.E. Hollowell and C.J. Murphy, *Langmuir*, **18** (2002), p. 10407.
18. Kim, Y., R.C. Johnson and J.T. Hupp, *Nano Letters*, **1** (2001), p. 165.
19. Zhu, M.Q., L.Q. Wang, G.J. Exarhos and A.D.Q. Li, *J. Am. Chem. Soc.*, **126** (2004), p. 2656.
20. Everett, D.H., (1988), *Basic Principles of Colloidal Science*, Royal Society of Chemistry, London, pp. 26–27.
21. Murray, C.B., D.J. Norris and M.G. Bawendi, *J. Am. Chem. Soc.*, **115** (1993), p. 8706.
22. Murray, C.B., C.R. Kagan and M.G. Bawendi, *Annu. Rev. Mater. Sci.*, **30** (2000), p. 545.
23. Zaitseva, N., Z.R. Dai, F.R. Leon and D. Krol, *J. Am. Chem. Soc.*, **127** (2005), p. 10221.
24. Sandhyarani, N. and T. Pradeep, *Int. Rev. Phys. Chem.*, **22** (2003), p. 221.
25. Chaki, N.K. and K.P. Vijayamohanan, *J. Phys. Chem. B*, **109** (2005), p. 2552.
26. Wang, S., H. Yao, S. Sato and K. Kimura, *J. Am. Chem. Soc.*, **126** (2004), p. 7438.
27. Prasad, B.L.V., S.I. Stoeva, C.M. Sorensen and K.J. Klabunde, *Chem. Mater.*, **15** (2003), p. 935.

edge over conventional materials. Such composite coatings are used in sensors (for protecting high-tech equipments from lasers in the form of optical limiters), nanoelectronics, catalysis and pharmaceuticals. These are also ideal systems used for probing the interfaces of the nanoparticle core and the shell, which is of fundamental relevance from the academic point of view. The term used to describe the synthesis of core-shell particles with well-defined morphologies and tailored properties is called 'particle engineering'. This is achieved by encapsulating the nanometal core within the shell of a preferred material, or by coating the nanoparticle core with the shell material. The shell protection imparts certain functional properties to the nanomaterial including: (1) monodispersity in size, (2) core and shell processibility, (3) solubility and stability, (4) ease of self-assembly, and (5) applications in nanoscale optics, nanoelectronics, as well as in magnetic, catalytic, chemical and biological fields. Shell protection is absolutely necessary for the following important reasons: (a) the shell can alter the surface charge, reactivity and functionality of the metal core thereby enhancing the stability and dispersibility of the colloidal materials; (b) by choosing a suitable shell-forming material, we can incorporate magnetic, optical and catalytic properties into the composite material; (c) encasing the metal core in a shell invariably protects it from physical and chemical changes; and (d) core-shells exhibit improved physical and chemical characteristics as compared to their single component counterparts. Various procedures have been employed for their synthesis, but the lack of suitable methodology for industrial production of core-shell nanomaterials has limited their applicability. A very critical aspect in the synthesis of such materials is the optimization of suitable/reliable synthetic parameters.

This chapter provides an overview of the various methods to synthesize core-shell nanoparticles, of their characterization using various spectroscopic and microscopic techniques, and their utility in material science, and relevance and future prospects, wherever necessary. The common characterization techniques involve UV-visible spectroscopy (UV-vis), transmission electron microscopy (TEM), powder X-ray diffraction (XRD), cyclic voltammetry (CV), etc.

The topic of core-shell nanoparticles can be divided into sub-sections depending on the nature of the core and the shell.

9.2 Types of Systems

9.2.1 Metal–Metal Oxide Core-shell Nanoparticles

These are among the most widely studied core-shell nanosystems. Nanosized metal clusters have intense colour, which can be tuned by varying the size of the clusters. One of the major problems associated with their handling is their vulnerability to aggregation. In order to avoid aggregation, various methodologies have been developed, with the most notable one being coating them with silica (Ref. 4), titania (Ref. 5), zirconia (Ref. 6) and maghemite (Ref. 7). Liz-Marzan, *et al.*, have developed a synthetic procedure to prepare silica-coated nanosized metal clusters, and the same methodology has been applied to various metals like Au, Ag and CdS (Ref. 8). The methodology uses 3-aminopropyl trimethoxy silane (APS), the silane coupling agent, which can bind to the nanoparticle surface and can also function as an anchor point

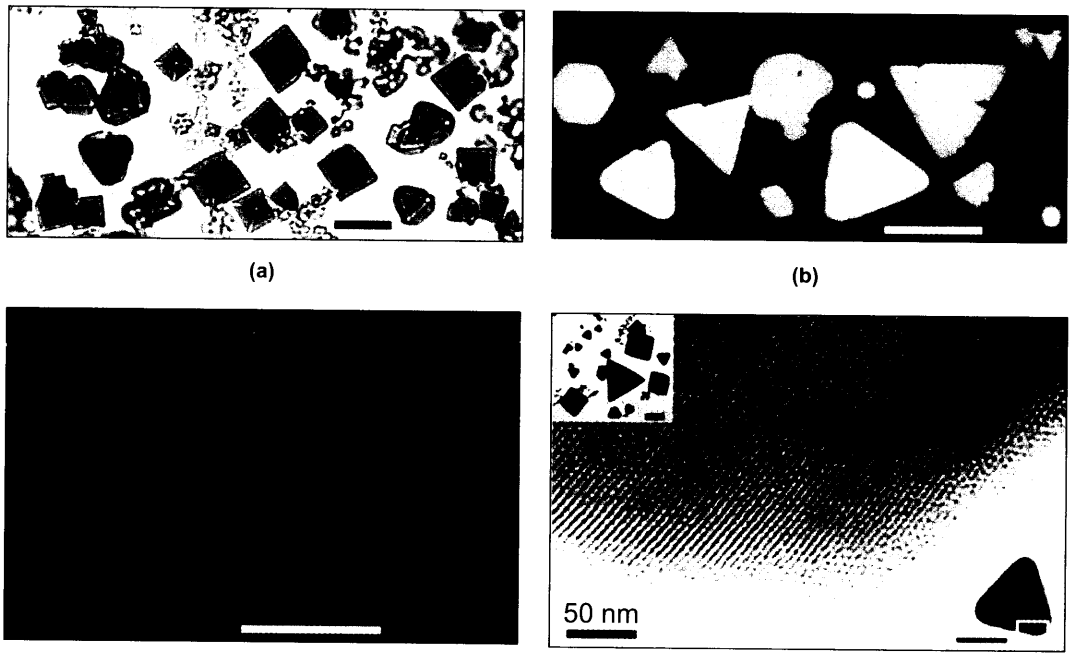

Fig. 8.14: *Superlattices built from a solution of CdSe crystals in nonanoic acid. (a) Optical micrograph of the superlattice and (b), (c) fluorescence microscopic images of the superlattices made from 3.5 and 5.3 nm nanocrystals, respectively. (d) TEM image taken from the edge of a superlattice made from 5.3 nm CdSe nanocrystals with the inset showing a low magnification image. Reprinted with permission from Zaitseva, et al. (Ref. 23). Copyright (2005) American Chemical Society.*

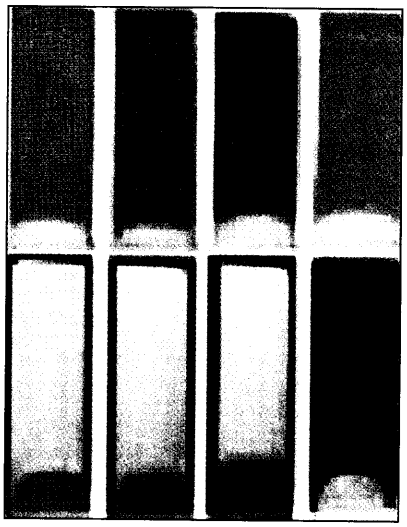

Fig. 9.15: *Transmitted and reflected colors from Au@SiO $_2$ multilayer thin films with varying silica shell thickness. Reprinted with permission from Ung, et al. (Ref. 49) Copyright (2001) American Chemical Society.*

pressure, D is comparable to the diameter ($2R$) of the particles. The coupling between the particles is very high at this point and the Coulomb gap disappears as shown in Fig. 8.18.

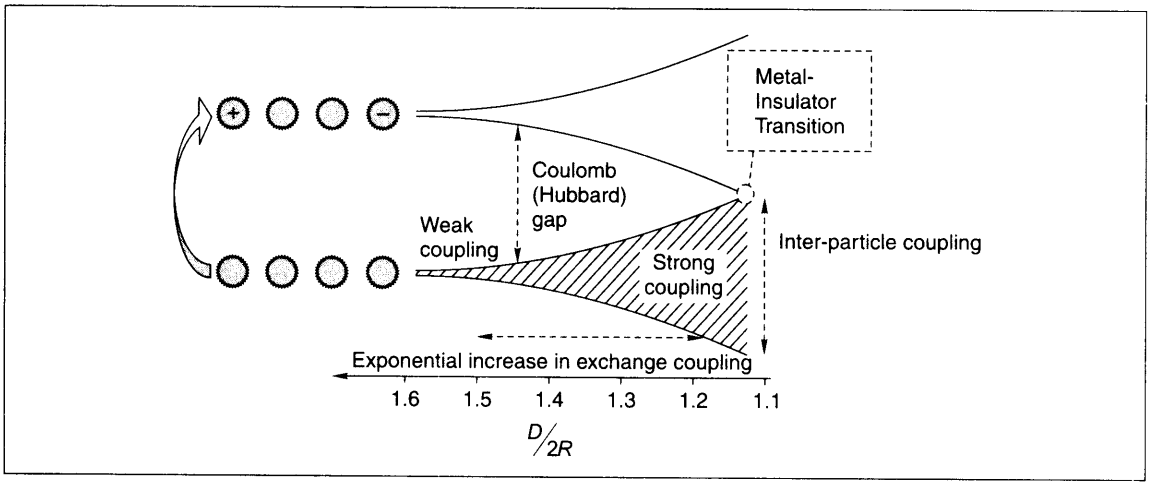

Fig. 8.18: *Schematic showing the metal insulator transition in superlattice. Reprinted with permission from the Annual Review of Material Science, Volume 30 © 2000 Annual Reviews. www.annualreviews.org©.*

Review Questions

1. Why nanoparticles need a protective layer of molecules?
2. What are the principal differences between a planar monolayer and a monolayer on a metal nanoparticle?
3. What are the principal properties of metal nanoparticles?
4. How would one characterize the monolayer and how can one characterize the core?
5. How do we know that a nanoparticle is indeed metallic?
6. Why most of the investigations are on gold particles?
7. What are the applications of gold particles?
8. What are the unique features of the Brust method?
9. What makes a metal cluster superlattice?
10. When does a metal cluster become a quantum dot? Are there examples?

Chapter 9

Core-shell Nanoparticles

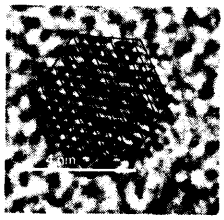

Core-shell nanoparticles are hybrid systems. They have a core and a shell. Various cores and diverse shells are available. The cores and shells can have distinct attributes such as metallicity, semiconductivity, magnetism, etc. Any combination of core and shell is possible. It is also possible to have one kind of core with the same kind of shell, namely a metallic core with another metallic shell, as Au@Ag, implying Au core and Ag shell. These systems are fascinating as they can protect the core from the chemical environment of the medium. A chemically active, biologically unsuitable core can be protected with an unreactive, chemically friendly shell. There are also several other possibilities. This chapter focuses on metallic cores.

Learning Objectives

- What are core-shell nanoparticles?
- Why do we need a core-shell system? What are the advantages of core-shell nanoparticles, in comparison to nanoparticles of core or shell?
- What are their optical, chemical and other properties? How can we understand these properties?
- What do we use them for?

9.1 Introduction

Controlled fabrication of nanomaterials has been one of the challenges faced by nanotechnologists and only limited progress has been achieved in this sphere so far. One of the fascinating characteristics of nanomaterials is that their properties are dependent on size, shape, composition and structural order. Therefore, it is imperative to develop effective and reliable methodologies to cater to the ever-increasing demands of tailored nanomaterials with the desired properties. Core-shell nanoparticles, i.e. particles with a well-defined core and a shell both in the nanometer range, have demanding applications in pharmaceuticals, chemical engineering, biology, optics, drug delivery and many other related areas in addition to chemistry.

During the past decade, there have been widespread research efforts to develop core-shell colloidal nanoparticles with tailored structural, optical, surface and other properties (Refs 1–3). Investigations on these types of materials have been catalyzed by their applicability in modern science and their technological

edge over conventional materials. Such composite coatings are used in sensors (for protecting high-tech equipments from lasers in the form of optical limiters), nanoelectronics, catalysis and pharmaceuticals. These are also ideal systems used for probing the interfaces of the nanoparticle core and the shell, which is of fundamental relevance from the academic point of view. The term used to describe the synthesis of core-shell particles with well-defined morphologies and tailored properties is called 'particle engineering'. This is achieved by encapsulating the nanometal core within the shell of a preferred material, or by coating the nanoparticle core with the shell material. The shell protection imparts certain functional properties to the nanomaterial including: (1) monodispersity in size, (2) core and shell processibility, (3) solubility and stability, (4) ease of self-assembly, and (5) applications in nanoscale optics, nanoelectronics, as well as in magnetic, catalytic, chemical and biological fields. Shell protection is absolutely necessary for the following important reasons: (a) the shell can alter the surface charge, reactivity and functionality of the metal core thereby enhancing the stability and dispersibility of the colloidal materials; (b) by choosing a suitable shell-forming material, we can incorporate magnetic, optical and catalytic properties into the composite material; (c) encasing the metal core in a shell invariably protects it from physical and chemical changes; and (d) core-shells exhibit improved physical and chemical characteristics as compared to their single component counterparts. Various procedures have been employed for their synthesis, but the lack of suitable methodology for industrial production of core-shell nanomaterials has limited their applicability. A very critical aspect in the synthesis of such materials is the optimization of suitable/reliable synthetic parameters.

This chapter provides an overview of the various methods to synthesize core-shell nanoparticles, of their characterization using various spectroscopic and microscopic techniques, and their utility in material science, and relevance and future prospects, wherever necessary. The common characterization techniques involve UV-visible spectroscopy (UV-vis), transmission electron microscopy (TEM), powder X-ray diffraction (XRD), cyclic voltammetry (CV), etc.

The topic of core-shell nanoparticles can be divided into sub-sections depending on the nature of the core and the shell.

9.2 Types of Systems

9.2.1 Metal–Metal Oxide Core-shell Nanoparticles

These are among the most widely studied core-shell nanosystems. Nanosized metal clusters have intense colour, which can be tuned by varying the size of the clusters. One of the major problems associated with their handling is their vulnerability to aggregation. In order to avoid aggregation, various methodologies have been developed, with the most notable one being coating them with silica (Ref. 4), titania (Ref. 5), zirconia (Ref. 6) and maghemite (Ref. 7). Liz-Marzan, *et al.*, have developed a synthetic procedure to prepare silica-coated nanosized metal clusters, and the same methodology has been applied to various metals like Au, Ag and CdS (Ref. 8). The methodology uses 3-aminopropyl trimethoxy silane (APS), the silane coupling agent, which can bind to the nanoparticle surface and can also function as an anchor point